Exploring Correlations: Natural Organic Matter (NOM) & Geophysical Signals

A case study at Lake Bolmen, Sweden

Ahmed Sabbir

Master of Science Thesis 30HP
ISRN LUTVDG/(TVTG-5183)/1-49/(2024)

Engineering Geology
Faculty of Engineering
Lund University

Exploring Correlations: Natural Organic Matter (NOM) & Geophysical Signals

A case study at Lake Bolmen, Sweden

Ahmed Sabbir

LUND UNIVERSITY

THESIS

Submitted to the Division of Engineering Geology, Faculty of Engineering, Lund University in Partial Fulfilment of the Requirements for the Degree of Master of Science in Water Resources Engineering

Lund 2024

Cover picture: Ahmed Sabbir

Lund University, Faculty of Engineering

Division of Engineering Geology

Exploring Correlations: Natural Organic Matter (NOM) & Geophysical Signals, A case study at Lake Bolmen, Sweden.

En undersökning av samband: Naturligt organiskt material och geofysiska signaler, En fallstudie vid sjön Bolmen, Sverige

Author: Sabbir, Ahmed

Supervisor(s): Barmen, Gerhard (Lund University); Martin, Tina (Lund University), Klante, Clemens (Sydvatten AB)

Examiner: Rosberg, Jan-Erik (Lund University)

ISRN LUTVDG/(TVTG-5183)/1-49/(2024)

Keywords: NOM, SIP, TOC, Fe, Correlation

Language: English

The work is performed within a collaboration between Lund University and Sydvatten AB

Digital edition Lund 2024

Abstract

Water, an essential element of life, is recently impacted by several issues, including climate change, affecting its quality. One of the changes in water quality is brownification, which results in water with a browner color. This yellow-brown color of water in a lake or any water surface can disrupt the treatment process and the aesthetics of the water body, thus increasing costs in the long run. In recent years, research on the brownification of water in lakes has come into focus, enhancing the opportunity to reduce vulnerability due to the presence of organic matter content in surface water. However, the correlation between Natural Organic Matter (NOM) in sediment and geophysical properties/signals has not yet been investigated. This thesis examines the correlations between geophysical signals derived from Spectral Induced Polarization (SIP) measurements and the concentrations of iron (Fe) and Total Organic Carbon (TOC). Sediment and water have been sampled from various locations in Lake Bolmen, situated in southern Sweden, primarily from ditches along its smaller tributaries. These samples have been subjected to analysis for multiple parameters, including TOC, Fe, dissolved oxygen, turbidity, color, and pH. Subsequently, the data were analyzed to investigate potential correlations. The results of this thesis suggest that there is no direct correlation between NOM in sediment and SIP signals. Although some weak correlations between certain SIP-measured data and NOM can be observed, they are not significant given the limitations of the analysis. However, assessing these relationships requires further investigation and long-term observation.

Sammanfattning

Vatten, en väsentlig beståndsdel av livet, riskerar i allt högre grad att förändras negativt av olika problem, inklusive klimatförändringar, vilket påverkar dess kvalitet. En av förändringarna i vattenkvaliteten är brunifiering, vilket innebär vatten med en brunare färg. En gulbrun färg på vatten i en sjö eller på en vattenyta kan störa behandlingsprocessen i vattenverk och minska vattnets estetiska värde, vilket ökar kostnaderna för dricksvattenförsörjning på lång sikt. På senare år har forskning om brunifiering av vatten i sjöar kommit i fokus och förbättrat möjligheten att minska sårbarheten på grund av närvaron av organiskt material i ytvatten. Emellertid har korrelationen mellan Naturligt Organiskt Material (NOM) i sediment och geofysiska egenskaper/signaler ännu inte undersökts. Detta examensarbete undersöker sambanden mellan geofysiska signaler härledda från mätningar av spektral inducerad polarisation (SIP) och koncentrationerna av järn (Fe) och Totalt Organiskt Kol (TOC). Sediment och vatten har provtagits från olika platser vid sjön Bolmen, belägen i södra Sverige, främst från diken längs dess mindre bifloder. Dessa prover har analyserats med avseende på flera olika parametrar, inklusive TOC, Fe, löst syre, turbiditet, färg och pH. Därefter analyserades data för att undersöka potentiella samband. Resultaten av denna undersökning antyder att det inte finns någon direkt korrelation mellan NOM i sediment och SIP-signaler. Även om vissa svaga samband mellan vissa SIP-mätdata och NOM kan observeras är de inte signifikanta med tanke på analysens begränsningar. Att slutligt bedöma dessa samband kräver dock ytterligare undersökningar och långvariga observationer.

Acknowledgement

The author of this thesis expresses his sincere gratitude to Sydvatten AB and the Engineering Geology Division of Lund University (LTH) for supporting the work through financial and collaborative support. This thesis is part of the Blue Transition project, supported by the Interreg North Sea, which aims to improve integrated water and soil management in the North Sea region in response to climate change.

Contents

List of Figures

List of Tables

List of Abbreviations

NOM	Natural Organic Matter
DOC	Dissolved Organic Carbon
DO	Dissolved Oxygen
POC	Particulate Organic Carbon
TOC	Total Organic Carbon
SIP	Spectral Induced Polarization
IP	Induced Polarization
Fe	Iron
pH	Potential of Hydrogen

1. Introduction

1.1 Background

Water, a fundamental elixir of life, is necessary for all sorts of life on earth. It is considered to be a vital element for achieving an adequate standard of living (United Nation, 2023). Although in recent decades, different factors, including climate-induced uncertainties (Frederick & Major, 1997) and human induced water stress (Mehran et al., 2017) have played a great role in exponentially degrading the 3% of available fresh water worldwide. It is apparent that the prioritization of ensuring the production of high-quality drinking water is of utmost importance. This entails an analysis of various factors, including cost and accessibility, along with a thorough evaluation of water sources and treatment methods to meet strict quality criteria.

The physical, biological, and chemical characteristics of water can help to ensure good quality (Arora, 2017). In recent decades, lake water in the northern hemisphere has shown an increase in trend in brownification, which results in a yellow-brown color of the surface water (Klante et al., 2021). Several studies have demonstrated a strong correlation between increased NOM concentration and increased brown water color, analyzing various factors such as Dissolved Organic Carbon (DOC) concentrations (Kritzberg, 2017), Iron concentration (Kritzberg & Ekström, 2012), and different drivers including climate change (Larsen et al., 2011), types of land use (Meyer-Jacob et al., 2015). Upon examining these data, it becomes evident that the primary cause of the brown coloration in water is the accumulation of Natural Organic Matter (NOM), a blend of diverse organic compounds of varying sizes stemming from soil decomposition. The brown color and higher NOM concentration are accompanied by undesirable consequences like; variable lake temperature (Bartosiewicz et al., 2019; Houser, 2006), higher cost in the drinking water treatment process (Cromphout et al., 2008). Therefore, it is important to mitigate the effects that are causing the change in water bodies, especially to reduce the drinking water treatment cost. Although there are plenty of studies available regarding NOM in surface water (Klante et al., 2022; Knap-Bałdyga & Żubrowska-Sudoł, 2023; Riyadh & Peleato, 2024), the correlation between NOM and different geophysical signal properties has not yet been investigated.

Geophysical methods involve applying physical principles to study the properties of underground by examining various materials' characteristics (Elias, 2013). Among the array of geophysical methods available for investigating different physical properties of subsurface geophysical features,

Seismic Reflection surveying, Electrical Resistivity methods, Geomagnetic methods, and Induced Polarization are commonly used. This thesis will focus on the utilization of the Induced Polarization (IP) method. IP measures the electrical conductivity and polarization of earth material; when it is measured over a wide range of frequency it becomes Spectral Induced Polarization (SIP) (Martin et al., 2021). In previous studies, the relationship between SIP and certain parameters such as textural configuration (Kruschwitz et al., 2010; Weller et al., 2010) and permeability (Revil et al., 2012) has been established. However, understanding the correlation between geophysical signals and NOM concentration is a new research field. This exploration holds significant potential in the SIP research domain, offering opportunities to develop new methods for investigating the presence and quality of NOM in soil and groundwater. Therefore, investigating the possibility of a connection between NOM and geophysical signals is important. Finding such a relationship could be highly helpful in streamlining decision-making and yielding insightful information.

In southern Sweden, Sydvatten AB produces potable water for seventeen municipalities, and twelve of them get water from Lake Bolmen (Sydvatten AB, 2021). Sydvatten AB has the right to extract a maximum of 6000 liters/sec water from the lake through the Bolmen tunnel (Sydvatten AB, 2024). Over the last decades, the water in this lake has been highly affected by brownification due to the increase in NOM, which comes with a higher cost for the treatment process (Klante et al., 2021). This thesis will focus on investigating any possible relationship between NOM in lake sediment and SIP measurement, which can potentially leads to a better understanding of NOM and SIP properties.

1.2 Objective

The objective of this thesis is to examine any possible correlation between NOM and SIP signals obtained in laboratory measurement. Overall aims of this research involves:

1. Investigate the possible relationship between the presence and concentration of Natural Organic Matter (NOM) in lake sediments and corresponding geophysical signals acquired through SIP analysis.
2. Investigate the possible relationship between the different parameters of lake water such as turbidity, color, pH, and Dissolved Oxygen (DO) with geophysical signals obtained by SIP analysis.

The outcome can help to identify which factors affect others, such as the dependent and independent variable when working with NOM and SIP signals in future studies. Also it could potentially lead to a better understanding of the brownification process when measuring ground geophysics.

Conversely, if no relationship is found, it will allow researchers to investigate other phenomena without being constrained by geophysics.

1.3 Delimitation

The outcomes of this thesis are delimited by several factors, primarily the heterogeneity of the collected samples, and limited number of samples acquired which hinders the development of statistically significant relationships. Consequently, it is recommended that future research consider these constraints to enhance the reliability and comprehensiveness of the results.

2. Study Area

2.1 Lake Bolmen

Lake Bolmen is situated at an altitude of 147 meters above sea level, and spans an area of 183 square kilometers, with a mean depth of 6.8 meters and a maximum depth of 36 meters. Exhibiting characteristics of the lake is an indication of oligotrophic conditions, and the trophic status of the lake is further distinguished by its humic nature. Moreover, the hydrological dynamics of Lake Bolmen are delineated by a water residence time of 1.6 years, reflecting its circulation patterns and exchange processes (Swedish Infrastructure for Ecosystem Science, 2023). The catchment area, encompassing 1640 square kilometers, comprises a heterogeneous landscape classified by 64% forest cover, 8% mire and wetland expanses, 15% lake coverage, 8% agricultural land use, and a residual 5% classified under other land categories (Swedish Meteorological and Hydrological Institute, 2023). Moreover, it is the 12th largest lake in Sweden, covering water supply for 600,000 people living in Skåne (Eklund et al., 2016).

The inflow of the lake is dominated by two tributaries, Storån and Lillån, coming from the north-western side. Storån drains around 30% of the drainage basin (Borgström, 2020). On the western side there is also a big inflow from the lake's Unnen outflow, called Lidhultsån. Different small tributaries and creeks like Murån, Ryds Å, Dannäsån, Smedjebäcken, Torarpsviken, and Lillasjöbäcken are contributing to the lake inflow, but in a small amount. Figure 1 shows the land use around the lake and some important inflows. Bolmen is well-known for its impressive range of plant and animal species, with a wide variety of fish and birds, as well as lush vegetation on the many islands. It is not only an important location for academic research but also a crucial source of clean drinking water for multiple municipalities and urban areas, thanks to the Ringsjöverket purification facility. Despite its ecological importance, there are ongoing challenges for achieving a satisfactory chemical water quality status. Pollutants like mercury compounds and brominated diphenyl ether, which come from various sources, including atmospheric deposition, continue to pose significant obstacles (Water Information System Sweden, 2024). For this thesis, locations from Lake Bolmen's catchments, mainly ditches along smaller tributaries, have been selected. Figure 2 shows the location of the sample collection sites. These locations are situated along two smaller streams named Ryds Å and Murån. Sections 2.2 and 2.3 provide further descriptions for considering these two smaller tributaries.

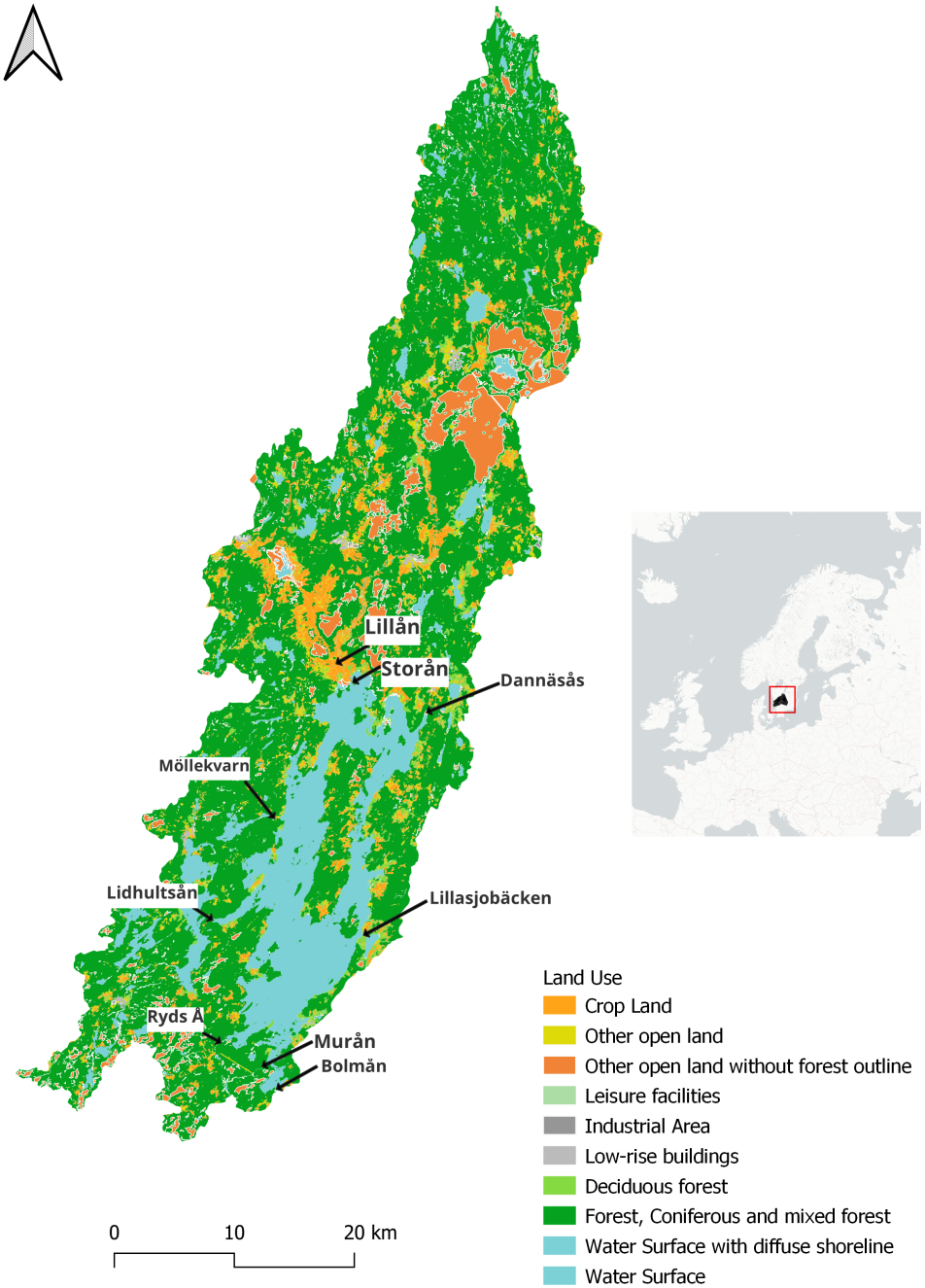

Figure 1: Geographic features surrounding Bolmen including selected tributaries and land use patterns.

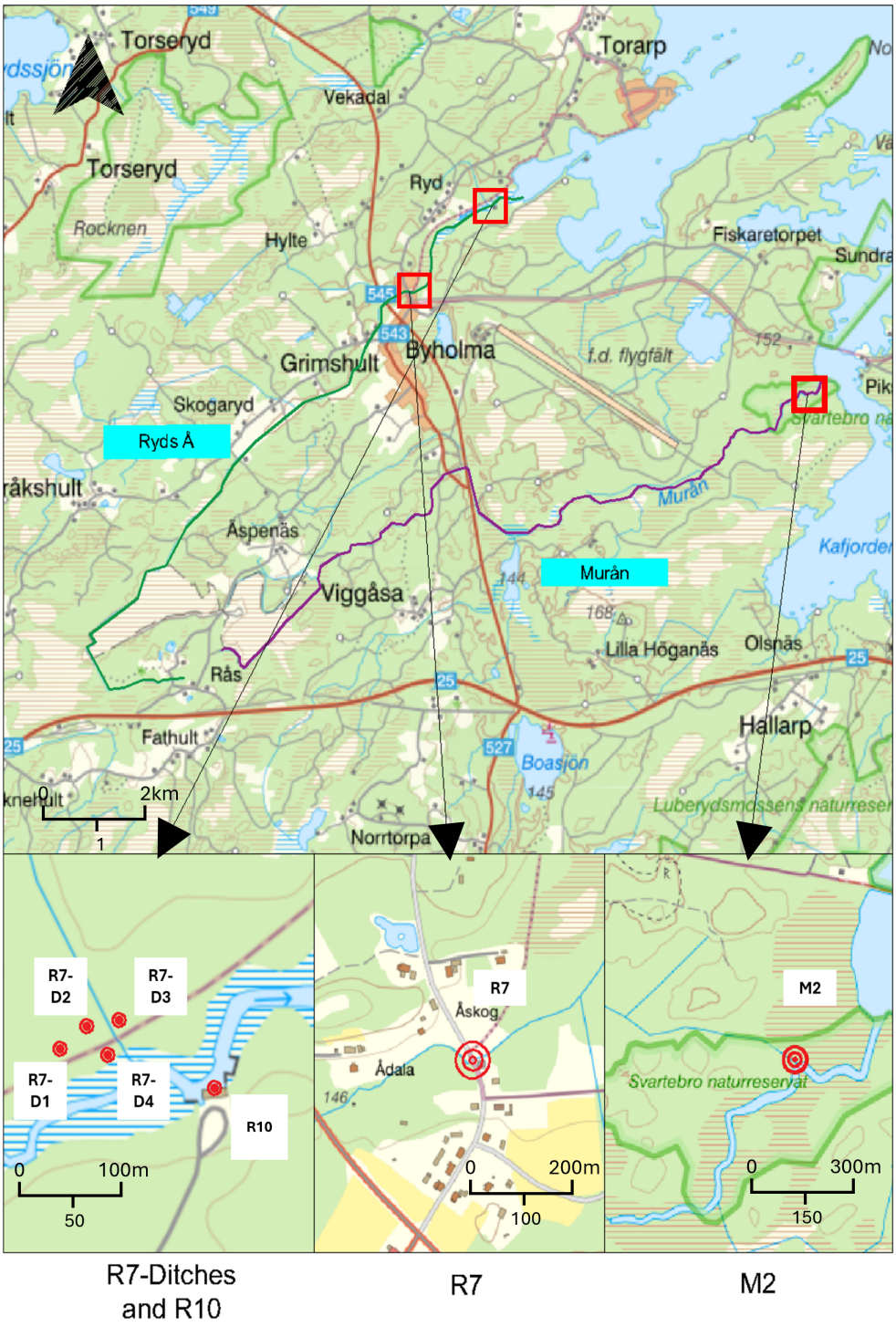

Figure 2: Flow path of streams Ryds Å and Murån with sample collection points. The green line represents the flow path of Ryds Å, and the purple line illustrates Murån's flow path. Sample collection points are marked with red circles for each location. Map is provided by Water Information System Sweden (2024).

2.2 Ryds Å

Ryds Å is a small stream originating from village Råås and passes Espenäsmosssen before it merges with Lake Bolmen. Since 1985, this location (Espenäsmosssen) has been utilized for peat extraction for energy purposes under the management of Södra Skogsägarna. The Kronoberg County Administrative Board has issued multiple permissions over the years, extending the current one until 2040 with an operational area of 66 hectares, this permit covers 188 hectares and permits the extraction of total 1.5 million cubic meters of peat, with an annual extraction of 0.07 million cubic meters according to Ström and Karlsson Öhman (2024). They mentioned that Ryds Å has a deeper color and the iron is an important contributor for the color. They also mentioned the necessity of studying the small ditches connected to it before flowing to Lake Bolmen. Therefore, in this thesis, four smaller ditches closer to the outlet have been taken into account. Further study is needed to verify the relation between peat extraction and browning in this particular area, but studies in general show that peat extraction can enhance the browning of surface water (Estlander et al., 2021; Härkönen et al., 2023). The sample collection points in Ryds Å include a total of six locations, comprising four ditches (R7-D1, R7-D2, R7-D3, and R7-D4), as well as locations R7 and R10. R7 and R10 are approximately 1500 meters apart from each other, and the four ditches intersect perpendicularly with R10, flowing towards Lake Bolmen. Figure 2 shows the detailed locations of the sampling points along Ryds Å, while Table 1 presents the coordinates of these locations with corresponding sample name for sediment and water samples.

Table 1: Coordinates of sampling location (SWEREF99)

Location	Lat (North)	Lon (East)	Sediment Sample	Water Sample
M2	6294127.00	416887.00	M2-S	M2-W
R10	6296019.00	413501.00	R10-S	R10-W
R7	6295115.00	412564.00	R7-S	R7-W
R7-D1	6296065.90	413364.43	R7D1-S	R7D1-W
R7-D2	6296075.73	413390.07	R7D2-S	R7D2-W
R7-D3	6296087.77	413414.63	R7D3-S	R7D3-W
R7-D4	6296073.24	413399.13	R7D4-S	R7D4-W

2.3 Murån

Flowing amidst the forest, Murån is a river that drains ditches into Bolmen from the southern side. According to the map by Geological Survey of

Sweden (2024), the surroundings of Murån resemble those of Ryds Å, characterized by peatlands. Grisaådran, a small tributary, also passes through Espenäsmosssen before joining Murån. Therefore, Murån has also been considered in this thesis. According to Klante et al. (2021), the difference in color and TOC at Murån shows significant changes from 2012 to 2018, compared to the other stations used in that study. The flow path of the streams Ryds Å and Murån can be seen in Figure 2.

3. Methodology

3.1 Data collection and Field Analysis

Data collection was carried out along two smaller streams that entered from Lake Bolmen's southern edge, as detailed in Section 2. Each data point in the sample was geo-referenced to determine its precise coordinates (Table 1). Each selected location is situated upstream from Lake Bolmen. While streams R7 and R10 had sufficient flow during the data collection period, stream M2 experienced low water levels, and all ditches (R7-D1, R7-D2, R7-D3, and R7-D4) were frozen in the top layer. Data collection occurred in February 2024, when the temperature was below -5°C. Sampling at these points involved collecting both sediment and water.

3.1.1 Sediment Sample

Two types of sediment samplers have been utilized for collecting samples from ditches and streams: the Kajak sediment sampler and the Ekman-Birge sampler. Using an acrylic tube that is 50 cm long and 5.5 cm in diameter, the Kajak sediment sampler gathers a complete sediment core sample (KC Denmark, 2022). The Ekman-Birge sampler, on the other hand, is a type of grab sampler that is usually intended for shallow water and can only capture the top sediment sample from the lake bed (Birge, 1922; Ekman, 1911). The Kajak sampler was used to collect samples from all the R7-Ditches, while the Ekman-Birge sampler was used for R10, R7, and M2 due to easier access to the locations. Both the samplers and the sample collection process are showed in Figures 17 and 18 of Appendix A. After the sample collection, the sediments are placed in airtight plastic containers to avoid any contact with air and stored in a freezer to minimize organic decomposition. Approximately 1.5 kgs of samples were collected at each spot, with most samples saturated with water.

3.1.2 Water Sample

Like the sediment samples, all water samples were collected consecutively to maintain consistency in the results. However, the water samples were collected before collecting the sediment sample to minimize sediment mixing in the water. Initially, the water quality parameters have been measured with the YSI EXO2 in the field. This device features seven sensor ports, a central wiper port, an optional depth sensor, and a battery compartment. It can measure 23 parameters simultaneously and is connected via Bluetooth to a computer (YSI, 2024). Though several parameters can be obtained from the sonde, for this thesis only four supposedly relevant parameters have been used, keeping in mind brownification and

possible NOM relation. The parameters that have been chosen are pH, DO (mg/L), Conductivity (μS/cm), and Turbidity (FNU). Three liters of water have been collected from each sampling site for the field test and laboratory test, and they are collected in airtight sample bottles that have been previously washed with distilled water.

3.1.2.1 *Conductivity*

Conductivity denotes a material capacity to conduct an electrical current. It is typically quantified in microsiemens per centimeter (µS/cm). Water conducts electricity due to the presence of ions and dissolved compounds. The higher the presence of ions and dissolved compounds, the higher the conductivity will be (Pal et al., 2015). Distilled water has a conductivity of 0.5–3 µS/cm (Atlas Scientific, 2024). In Sweden, the typical conductivity of lake is between 20 µS/cm to 200 µS/cm (Göta älvs vattenvårdsförbund, 2016).

3.1.2.2 *Turbidity*

Waters clarity can be determined by measuring turbidity. Turbidity in surface waters is primarily caused by the reflection of particle surfaces, which affects the path of incoming light as it passes through the sample. (Swedish University of Agricultural Sciences, 2023). Turbidity of water can accomplish certain changes in aquatic environment (Secondi et al., 2007), but it is not necessarily indicated as a water quality parameter because high turbid water does not always represent poor quality water (US EPA, 2021), but it can increase the treatment cost for certain circumstances (Davis et al., 2010).

3.1.2.3 *Dissolved Oxygen*

The parameter of Dissolved Oxygen (DO) is important in assessing the quality of the water. For example, DO levels below 5 mg/L are insufficient for fish to survive in water, and this indicates possible contamination (Bozorg-Haddad et al., 2021). According to Knoll et al. (2018), long-term browning in the water can lower the dissolved oxygen content in an oligotrophic lake. In order to determine if DO and SIP signals are interdependent, DO has been assessed in mg/L.

3.1.2.4 *pH*

Since pH provides information about a water's biological, chemical, and physical characteristics, it is regarded as a crucial water quality metric. Dissolved Organic Carbon (DOC) in water acts as a weak acid, thus it

help to regulate acidity in water by acting as a buffer when strong acid is added in certain cases (Winterdahl et al., 2014). Klante et al. (2021) demonstrated that organic matter tends to dissolve more readily in water during the winter and spring when pH levels are lower, possibly resulting in a more vivid coloration in the summer when rainfall increases. In addition, increased precipitation in summer may further raise lake pH levels.

3.2 Laboratory Analysis

In this thesis, laboratory analysis has been conducted to thoroughly examine sediment and water samples. A portion of the collected sediment sample (1 kg) has undergone testing for Total Organic Carbon (TOC) and iron (Fe) contents, while the remaining 0.5 kg has been utilised for Spectral Induced Polarisation (SIP) analysis. TOC and Fe contents have been analyzed in an accredited laboratory of SGS Analytics AB. During the same time as the sediment sample, SIP analysis has also been conducted for the water sample. It is important to mention that, the conductivity and pH of the water sample have also been measured in lab using a multimeter. As the temperature of the lab was 25°C, the conductivity increased as the temperature was much higher than that of the field (Hermans et al., 2014). On the other hand, pH has decreased as the temperature increased for all samples (Zaidi & Pal, 2015).

3.2.1 TOC and Iron contents

3.2.1.1 *Total Organic Carbon (TOC)*

Total Organic Carbon (TOC) represents all molecular organic carbon species found in water source (Thurman, 1985). After removing the part of inorganic carbon by acidification, TOC can be defined as the sum of DOC (Dissolved Organic Carbon) and POC (Particulate Inorganic Carbon) (Sillanpää et al., 2015). Although TOC and DOC both can be used as important parameters in Natural Organic Matter (NOM) removal in wastewater treatment, their average differences in values are only about 5% (Gadmar et al., 2002; Köhler, 1999). Therefore, TOC and DOC is closely identical in measures. Additionally, TOC represents color with a strong connection and is consistent with color values (Finstad et al., 2016; Klante et al., 2021).
The TOC measurement of the sediment sample has been done according to the standard prEN 17505:2020. This test involves the dry combustion method in the presence of oxygen at varying temperatures ranging from 150-900°C.

3.2.1.2 *Iron (Fe)*

Iron contributes to an essential part of freshwater, as its presence in water is closely linked to its specific chemical form, providing availability and mobility (Sharma et al., 2010). NOM can react with Fe ions and form soluble complexes, affecting the aquatic environment (Karlsson & Persson, 2012). Previous studies have found that iron also contributes to change water color (Ekström, 2013; Weyhenmeyer et al., 2012).
Fe in the sediment sample has been measured according to the standard of EN 16171/ EN 16173 mod, which can outline various elements in sludge, sediment, and soil. In order to dissolve the solid materials and liberate the components of interest, this approach entails digesting the medium with nitric acid. Following the digestion, the elements' amounts are determined using analytical methods suitable for each element (CEN, 2005).

3.2.2 Spectral Induced Polarization

Both sediment and water samples have been analyzed with Spectral Induced Polarization (SIP). SIP determined the complex resistivity of material by measuring impedance magnitude and phase shift. This complex resistivity can be inverted and divided into an omic part also denoted as real part of conductivity and a polarization part also known as imaginary part of conductivity. SIP measurements is usually taken over a board range of frequency. The complex electrical resistivity can be denoted by:

$$\frac{1}{\rho^*(\omega)} = \sigma^*(\omega) = |\sigma| e^{i\varphi(\omega)} = \sigma'(\omega) + i\sigma''(\omega) \tag{1}$$

Here, $\rho^*(\Omega\text{m})$ is the complex resistivity, σ^* (S/m) is the complex conductivity, $|\sigma|$ (S/m) represents the magnitude of conductivity, φ (rad) is the phase angle, σ' (S/m) is the real part of conductivity, and σ'' (S/m) is the imaginary part of the conductivity. $\omega = 2\pi f$ (Hz) is the angular frequency, and $i = \sqrt{1}$ represents the imaginary number.
The characterization of a material's electrical properties involves the distinction between its real (σ') and imaginary (σ'') conductivity components, each representing unique phenomena. The real part, shows how conductivity changes with frequency and includes the flow of electricity through the pores and across particle surfaces, showing both electrolytic and surface conductivity. In contrast, the imaginary component is associated with phenomena related to the storage or redistribution of electrical charge rather than the direct flow of electric current. It records polarisation effects across the frequency spectrum caused by charged surfaces, showing that the sediment can hold charge and reflect different electrical properties (Reynolds, 1997). To explain the obtained SIP data, inversion modeling is used. The most common one for data inversion is Cole-Cole model (Cole & Cole, 1941). By fitting the data, several parameters can be

generalized, like conductivity (ρ), relaxation time (τ), and chargeability (m). In Cole-Cole model the complex impedance $Z^*(\omega)$ can be written as:

$$Z^*(\omega) = R_0 \left[1 - m_0 \left(1 - \frac{1}{1 + (\omega\tau i)^c} \right) \right] \quad (2)$$

Here, R_0 is the low frequency resistance, τ, c, and m_0 are Cole-Cole parameters and $i = \sqrt{1}$ is imaginary number. These parameters can be obtained by fitting the data into a inversion model.
Like Cole-Cole model, there are several other empirical models available to fit the data with higher accuracy. One of them is Debye Decomposition (Nordsiek & Weller, 2008). This model solve the problem of assuming a single relaxation peak for Cole-Cole model. Debye Decomposition can compose several Debye models, allowing larger spectral shape with multiple relaxation peak.
In this thesis the data acquired from the SIP analysis has been fitted to both Cole-Cole model and Debye Decomposition. From the fitted parameter, complex resistivity ρ_{cc} (Ωm) has been taken from the Cole-Cole parameter, on the other hand relaxation time τ_{DD} (s), and chargeability m_{DD} have been taken from the Debye Decomposition.

3.2.2.1 *Sample Preparation for SIP Analysis*

All samples have been prepared in the laboratory before starting SIP measurement. In order to eliminate air from the sample holder and reduce erroneous readings, the sediment has been tamped with a tamping bar. For the sediment and water samples, two different sample holders have been used. Every sample holder has been cleaned and dried to eliminate any contamination prior to the measurement. The weight of the sediment and water was measured by subtracting the empty weight from the loaded weight of the sample holder. The weights of sediment and water used for SIP analysis are listed in Table 2. It is important to mention that the water and sediment used in the sample preparation process were not filtered or altered to maintain the same condition as in the field. Therefore, some roots were found in the sediment sample, while some algae and suspended particles were found in the water sample.

3.2.2.2 *Instrument for SIP*

A portable SIP unit (PSIP) from Ontash and Ermac, Inc. has been utilised for SIP measurements (Ontash & Ermac, n.d.). Phase shift (φ) and impedance magnitude ($|Z|$) have been measured at a range of frequencies, spanning from 10000 Hz to 0.001 Hz. An amplitude of 5V and a number of steps of 71 have been utilised for the maximum sweep settings. The amplitude is measuring the maximum voltage reach by the imposed electrical signal and number of steps is measuring number of frequency steps.

Table 2: Sediment and water sample weight measured prior to the SIP measurements

Name	Sediment (g)	Water (g)	Temp. (°C)
M2	84.6	78.5	25.7
R10	102.5	78.7	21.4
R7-D1	86.7	78.8	24.7
R7-D2	78.9	78.5	25.9
R7-D3	81.6	77.9	26.9
R7-D4	86.8	79	20.4
R7	133	79	22.6

With an integration time and cycle of 5 sec, the settle time and cycle have been set to 1 sec. The settle time and settle cycles parameters determine the duration before measurements commence. Meanwhile, the integration time and integration cycles parameters control the duration designated for measurement periods. The aforementioned configurations are only applicable for the main measurement that was considered throughout the study. Nevertheless, three more measurements were taken over a shorter period of time were used to verify the integrity of the main measurement. Figure 3 is showing a laboratory setup for SIP measurement and water conductivity test by multi meter. In Figure 21 of Appendix C the block diagram of the PSIP unit is provided for further details.

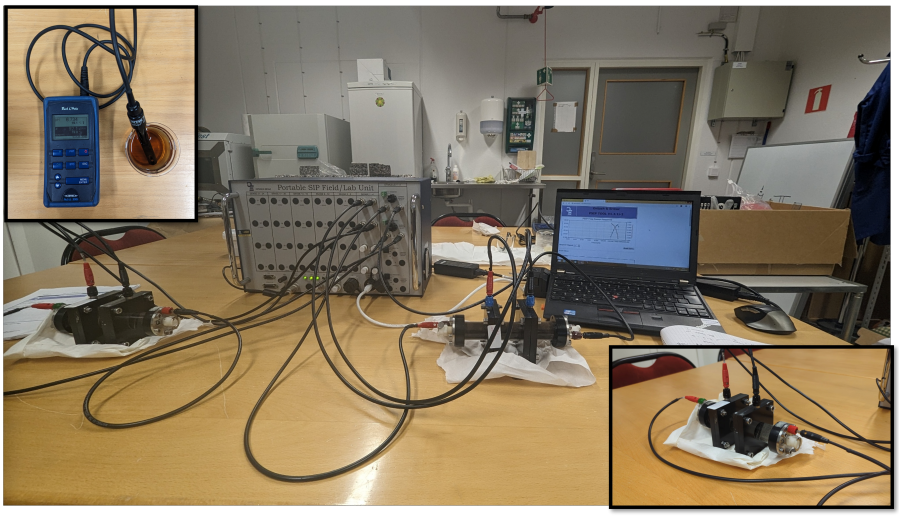

Figure 3: Laboratory setup for SIP analysis (Multimeter in top left; Sample holder arrangement in bottom right)

3.2.2.3 *Data Analysis from SIP*

From the PSIP unit, Impedance Z (Ω) and Phase shift φ (rad) have been obtained. After that, phase shift φ (rad) has been converted to negative

phase shift $-\varphi$ (mrad) and impedance in resistivity ρ (Ωm) has been obtained by multiplying k= 0.006138 with impedance (Ω). The equation for computing resistivity ρ is as followed.

$$\rho = \frac{V}{I} * k \tag{3}$$

where, $\frac{V}{I}$ represent the impedance Z (Ω) and k represent geometric factor for the sample holder. From resistivity, real part of conductivity σ' (S/m) and imaginary part of conductivity σ'' (S/m) can be calculated. Before analyzing, data at frequencies above 10^3 Hz were cut off to neglect epsilon effects (Wang & Slater, 2019), because this effect can be seen at high frequencies, where the dielectric properties of the materials, specifically the dielectric permittivity, become significant. Occasionally occurring 50 Hz noise has also been omitted to neglect coupling effect. The analysis includes frequency from the range of 10^{-2} Hz to 10^3 Hz.

The data analysis has been carried out with python3 with the help of numpy and scikit-learn package. Non-weighted linear regression has been used to find the correlation considering similar weight and simple random sampling. The trend lines in the correlation graphs are calculated to match the best according to dependent and independent values, but do not necessarily indicate that, the model is good or bad predictor. The curve fitting of the SIP analysis into Cole-Cole model and Debye Decomposition model has been done by pyGIMLi (Rücker et al., 2017). It is an advanced open source package for multi-method modelling and inversion application of data in geophysics.

3.2.2.4 *Porosity Calculation*

The porosity of the sediment sample after placing it in the sample holder has been calculated according to Archie's law (Archie, 1942).

$$C_t = \frac{1}{a} C_\omega \phi^m S_w^n \tag{4}$$

where, C_t is the electrical conductivity for sediment (saturated with water), C_ω is the conductivity of water, m = 2 is cementation factor (assumed), a = 1 is tortuosity factor (assumed), and S_w= 1 is the fluid saturation of the pores, and n = 1 (assumed) is the saturation exponent. Equation 4 can also be written as:

$$\frac{\rho_0}{\rho_w} = a\phi^{-m} S_w^{-n} \tag{5}$$

Here, $\frac{\rho_0}{\rho_w}$ represents the formation factor F. ρ_0 is the resistivity of sediment and ρ_w is the resistivity of water found from the SIP analysis after fitting the data in to Cole-Cole model. $S_w^{-n} = 1$ when the pore is water saturated.

So, the formation factor F can be calculated as:

$$F = \frac{a}{\phi^m} = \frac{\rho_0}{\rho_w} \tag{6}$$

From Equation 6 the porosity of the sample ϕ can be calculated for every sample. Calculated values are shown in Table 5 of section 4.3.3.

4. Results

The results of this thesis is divided into different parts for investigating relations. Related parameters of SIP analysis (ρ_{cc}, τ_{DD}, m_{DD}, σ', σ'') have been compared with TOC, Fe, Water Color, Dissolved Oxygen, Turbidity and pH. In addition resistivity (ρ_{10}) and negative phase shift ($-\varphi_{10}$) data at a selected frequency of 10 Hz have also been taken into consideration randomly to check with the fitted results and also to find correlation with different NOM parameters.

4.1 Spectral Properties of SIP Measurements

This section compares the measured data from the SIP analysis (before fitting to the inversion model). Here, the resistivity and negative phase shift are shown over the entire measured frequency range. Figure 4 shows the resistivity of all sediment and water samples together. It can be seen that, for all sediment samples, the value of resistivity is higher than that of water. All the samples fall in the range of 150 to 250 Ωm except R7, which is more than 300 Ωm. Figure 5 shows that, all sediment samples exhibit larger phase shift effects, whereas the water sample shows almost no phase shift. For sample R10, R7-D1, and R7 relatively low epsilon effects can be seen on higher frequency.

The comparison of frequency vs resistivity and phase shift of sediment samples are depicted in Figure 6 and for water sample in Figure 7. Among the sediment samples R7 is showing the highest value of resistivity of 320 Ωm and M2 is showing the lowest around 145 Ωm (Figure 6a). For water samples in Figure 7a R7-D2 has the highest value of around 170 Ωm and R10 has the lowest value of around 75 Ωm. It is evident from Figure 6b that all sediment samples exhibit a peak in negative phase shift within the frequency range of 30–40 Hz. This range can be considered a peak frequency, where a local maximum occurs. At frequency above 100 Hz, all samples except R10 and R7 are influenced by higher-frequency effects. In contrast, the negative phase shift of all water samples remains at close to zero (Figure 7b).

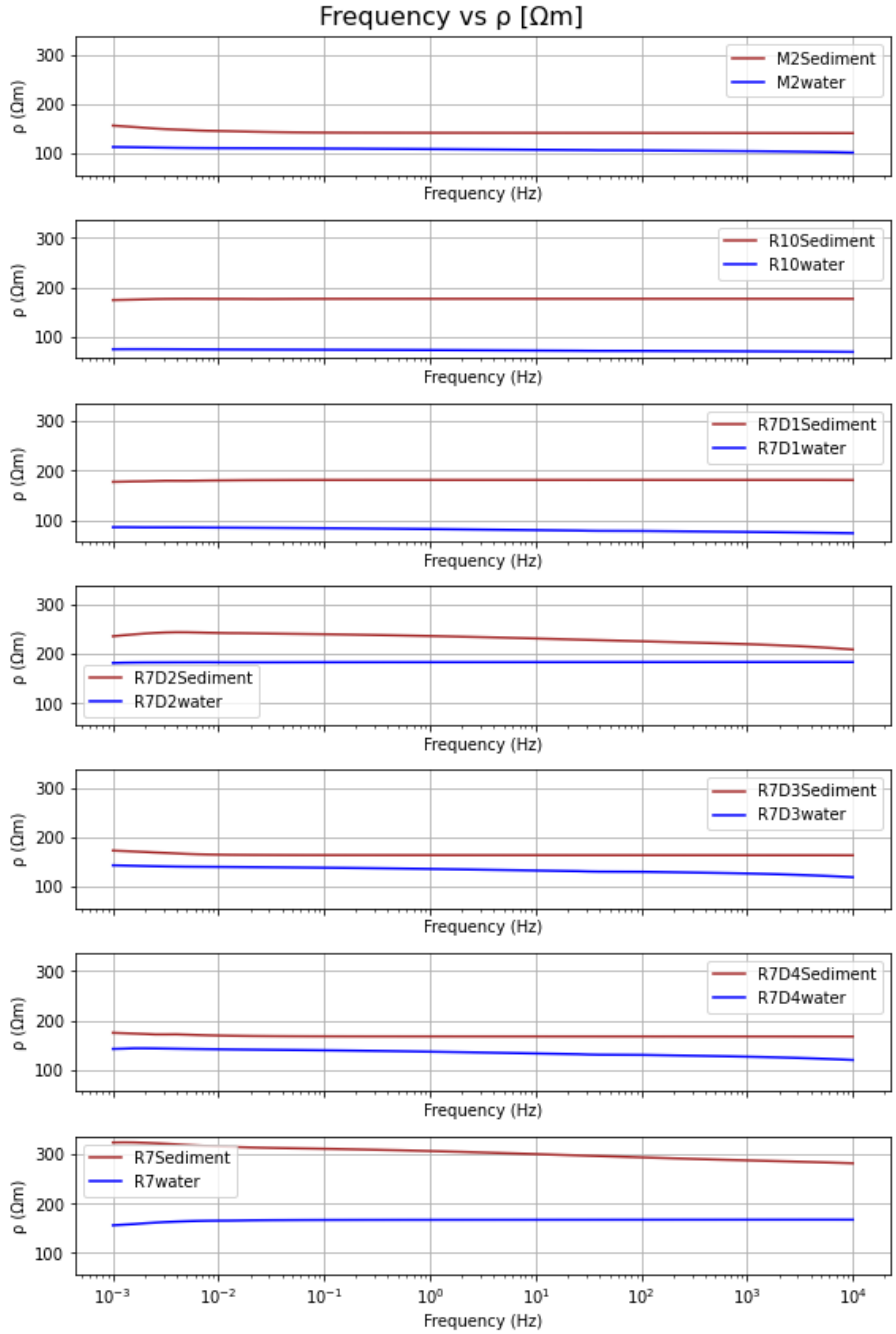

Figure 4: Frequency vs resistivity plots of all sediment and water samples. Legends showing the sampling location with respect to the sample types. The figure is showing the entire frequency range that have been measured.

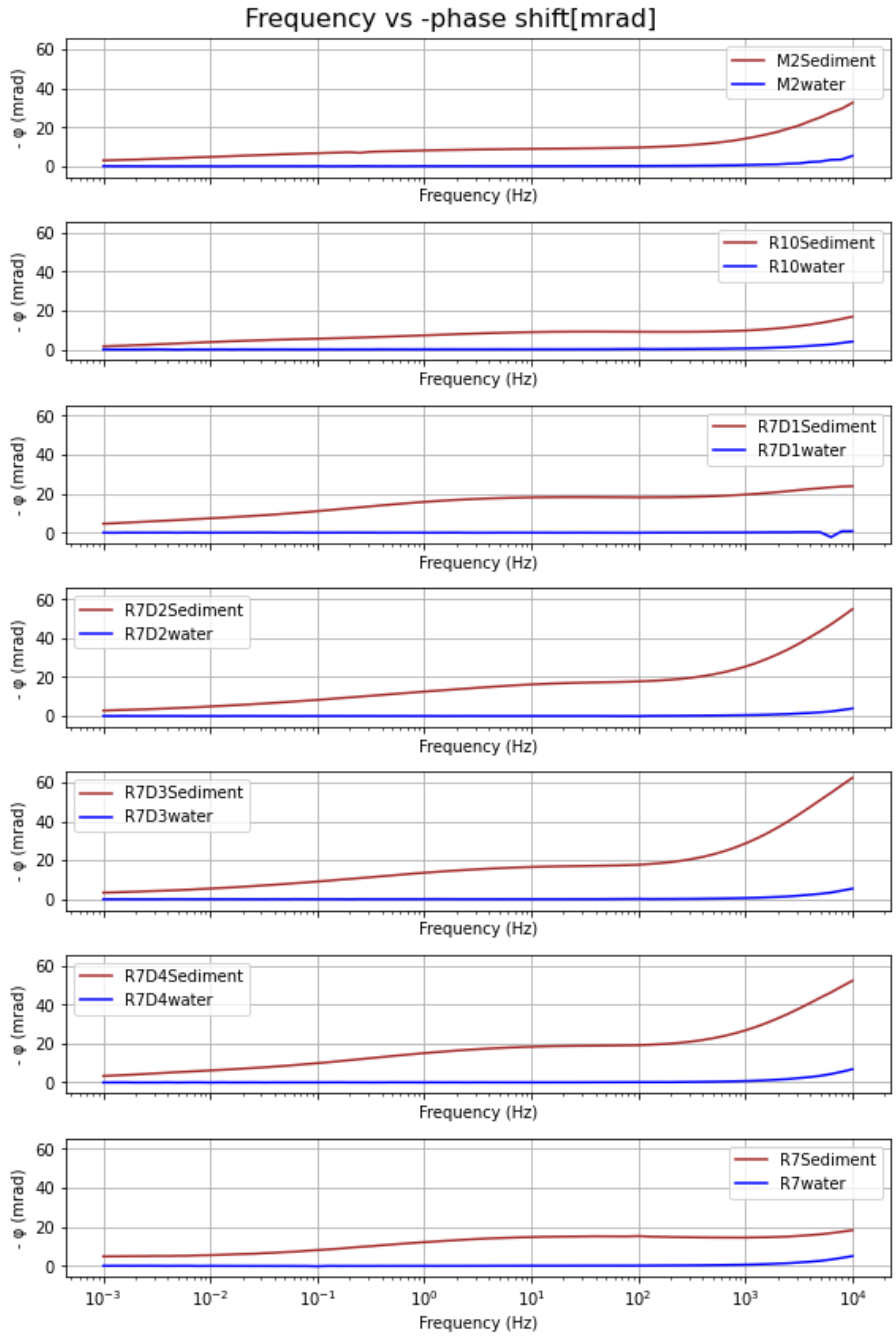

Figure 5: Frequency vs negative phase shift graphs of all sediment and water samples. Legends showing the sampling location with respect to the sample types. The figure is showing the entire frequency range that have been measured.

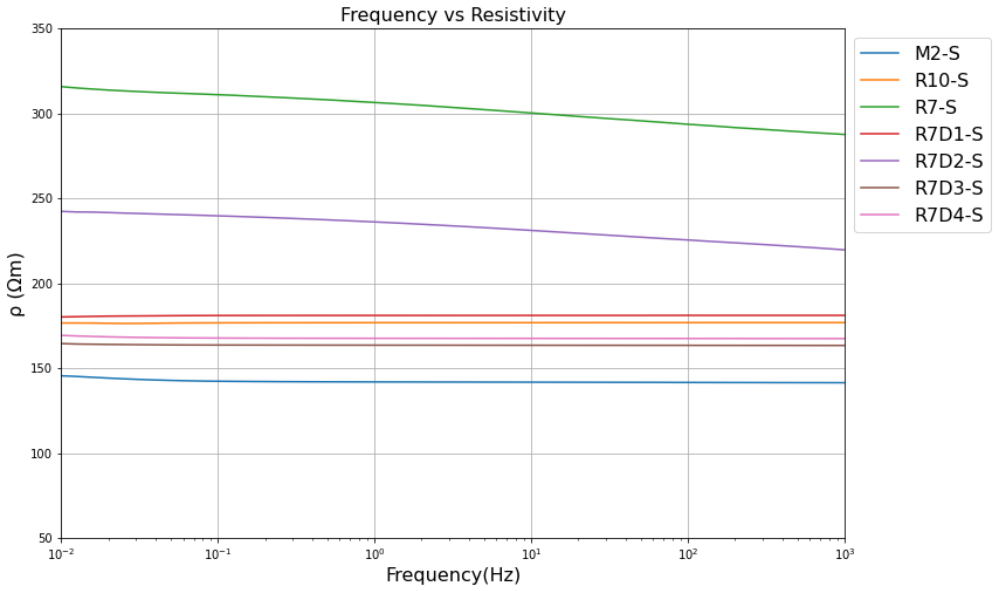

(a)

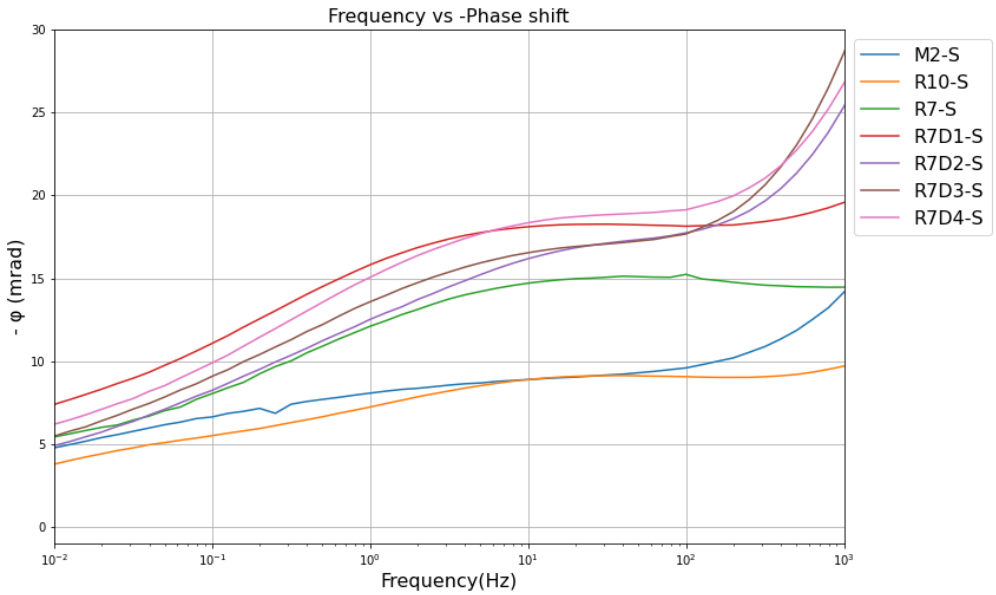

(b)

Figure 6: Frequency vs resistivity and negative phase shift of sediment samples. Figure (a) is showing the results obtained from frequency vs resistivity and Figure (b) is showing the results obtained in from frequency vs negative phase shift of sediment samples. Entire range of frequency is considered for this figure.

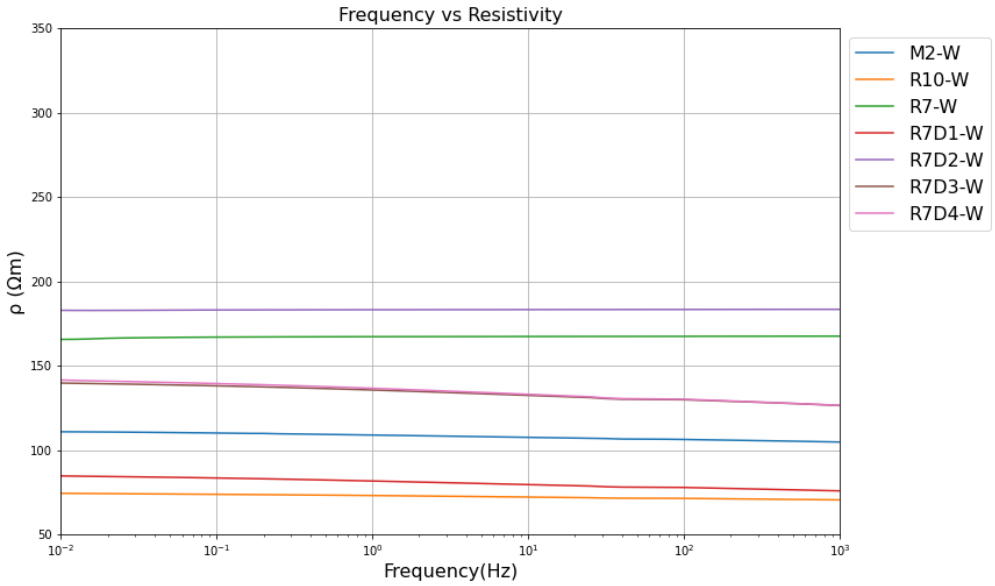

(a)

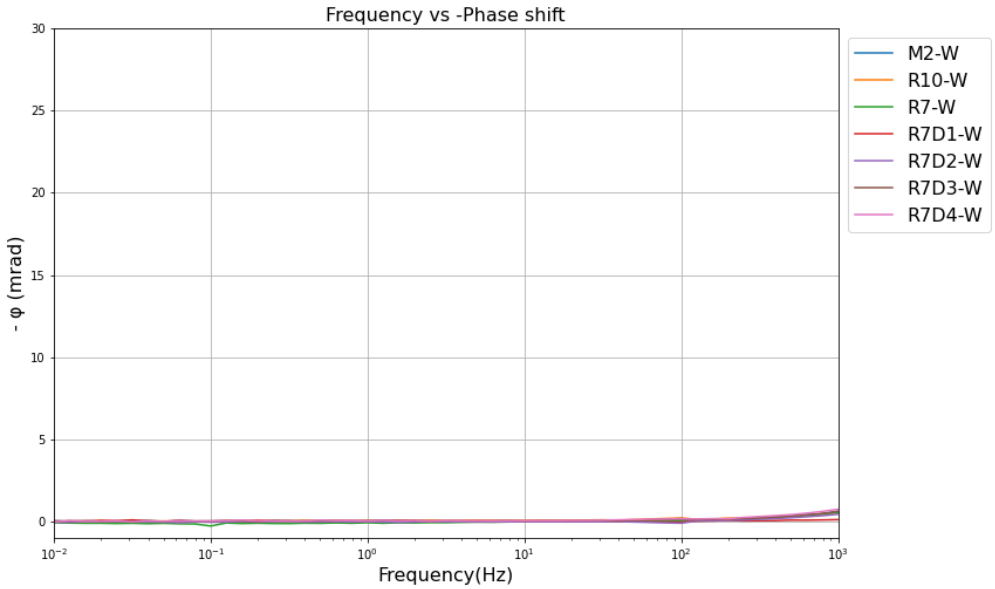

(b)

Figure 7: Frequency vs resistivity and negative phase shift of water samples. Figure (a) is showing the results obtained from frequency vs resistivity and Figure (b) is showing the results obtained in from frequency vs negative phase shift of water samples. Entire range of frequency is considered for this figure.

4.2 Data fitting

As discussed in section 3.2.2, the SIP data has been fitted to Cole-Cole model and Debye Decomposition model. The fitting results have been used to obtain ρ_{cc}, τ_{DD}, and m_{DD}. Table 3 is showing the values of fitted parameters. Every sediment and water sample has gone through fitting, but in Figures 19 and 20 of Appendix B one fitted data from location (M2)

has been shown as example to reduce complexity. Figure 19 is showing the fitted curve of sediment sample for location M2 and Figure 20 is showing the fitted curve of water sample for location M2.

Table 3: Fitted data (ρ_{cc}, m_{DD}, τ_{DD}) and Laboratory data (σ', σ'', ρ_{10}, $-\varphi_{10}$) for all analyzed sediment and water samples

Type	Sample	ρ_{CC} (Ωm)	m_{DD}	τ_{DD} (s)	σ' (S/m)	σ'' (S/m)	ρ_{10} (Ωm)	$-\varphi_{10}$ (mrad)
Sediment	M2-S	148.5	0.06	4×10^{-3}	7.0×10^{-3}	6.2×10^{-5}	141.7	8.8
	R10-S	184.5	0.01	3×10^{-5}	5.6×10^{-3}	5.1×10^{-5}	176.7	8.8
	R7D1-S	198.1	0.05	2×10^{-5}	5.5×10^{-3}	1.1×10^{-4}	181.2	18.1
	R7D2-S	246.6	0.16	1×10^{-3}	4.3×10^{-3}	7.0×10^{-5}	231.1	16.1
	R7D3-S	172.7	0.10	2×10^{-5}	6.1×10^{-3}	1.0×10^{-4}	163.4	16.5
	R7D4-S	180.0	0.09	1×10^{-4}	6.1×10^{-3}	1.0×10^{-4}	163.4	16.5
	R7-S	323.7	0.10	6×10^{-3}	3.3×10^{-3}	4.8×10^{-5}	300.2	14.7
Water	M2-W	107.6	0.07	7×10^{-3}	9.3×10^{-3}	1.4×10^{-7}	107.4	0.02
	R10-W	72.2	0.06	16×10^{-3}	12.5×10^{-3}	1.2×10^{-7}	72.4	0.06
	R7D1-W	79.7	0.12	16×10^{-3}	5.4×10^{-3}	4.9×10^{-8}	79.4	0.01
	R7D2-W	183.2	0.001	18×10^{-3}	7.5×10^{-3}	2.5×10^{-7}	183.2	-0.01
	R7D3-W	132.2	0.12	7×10^{-3}	7.5×10^{-3}	2.5×10^{-7}	132.3	0.03
	R7D4-W	133.0	0.13	11×10^{-3}	7.5×10^{-3}	3.4×10^{-7}	132.9	0.05
	R7-W	167.2	0.002	18×10^{-3}	5.97×10^{-3}	5.9×10^{-9}	167.2	0.01

4.3 Comparison of NOM and SIP parameters for sediment samples

Results obtained from the NOM and sediment sample analysis has been presented in this section. The process of data preparation and methods involved in it has been described in 3.2. Table 4 is showing the TOC and Fe contents obtained from the laboratory analysis and Table 3 is showing all the necessary SIP data used in this analysis.

Table 4: TOC and Fe contents of sediment samples obtained from laboratory analysis. TOC is measured in (%) of Total Solids (TS) and Fe is measured in mg/kg

Sample	**TOC (% of TS)**	**Fe (mg/kg)**
M2-S	56	600
R10-S	2.7	5200
R7D1-S	53	12000
R7D2-S	59	1400
R7D3-S	58	2200
R7D4-S	18	7700
R7-S	5.3	3000

4.3.1 TOC vs SIP parameters of Sediment Sample

The Total Organic Carbon (TOC) has been compared with various parameters derived from Spectral Induced Polarization (SIP) analysis. Resistivity (ρ_{10}), negative phase shift ($-\varphi_{10}$), real part of conductivity (σ'), and imaginary part of conductivity σ'' are derived from raw data at a frequency of 10 Hz. Simultaneously, resistivity (ρ_{CC}) and chargeability (m_{DD}) are extracted from the fitted data obtained through the Cole-Cole and Debye Decomposition models, respectively.
Figure 8 is illustrating TOC vs different parameters of SIP analysis. The results of all the parameters are relatively dispersed and it is really hard to see any relationship. Most of the data is clustering especially the R7D1-S, R7D2-S, R7D3-S and M2-S. Compared to other values, imaginary conductivity is showing higher R^2 value of 0.23, but it is not sufficient to show a concrete relation. Therefore, a correlation between the fitted SIP parameters and the TOC of Sediment could not be found.

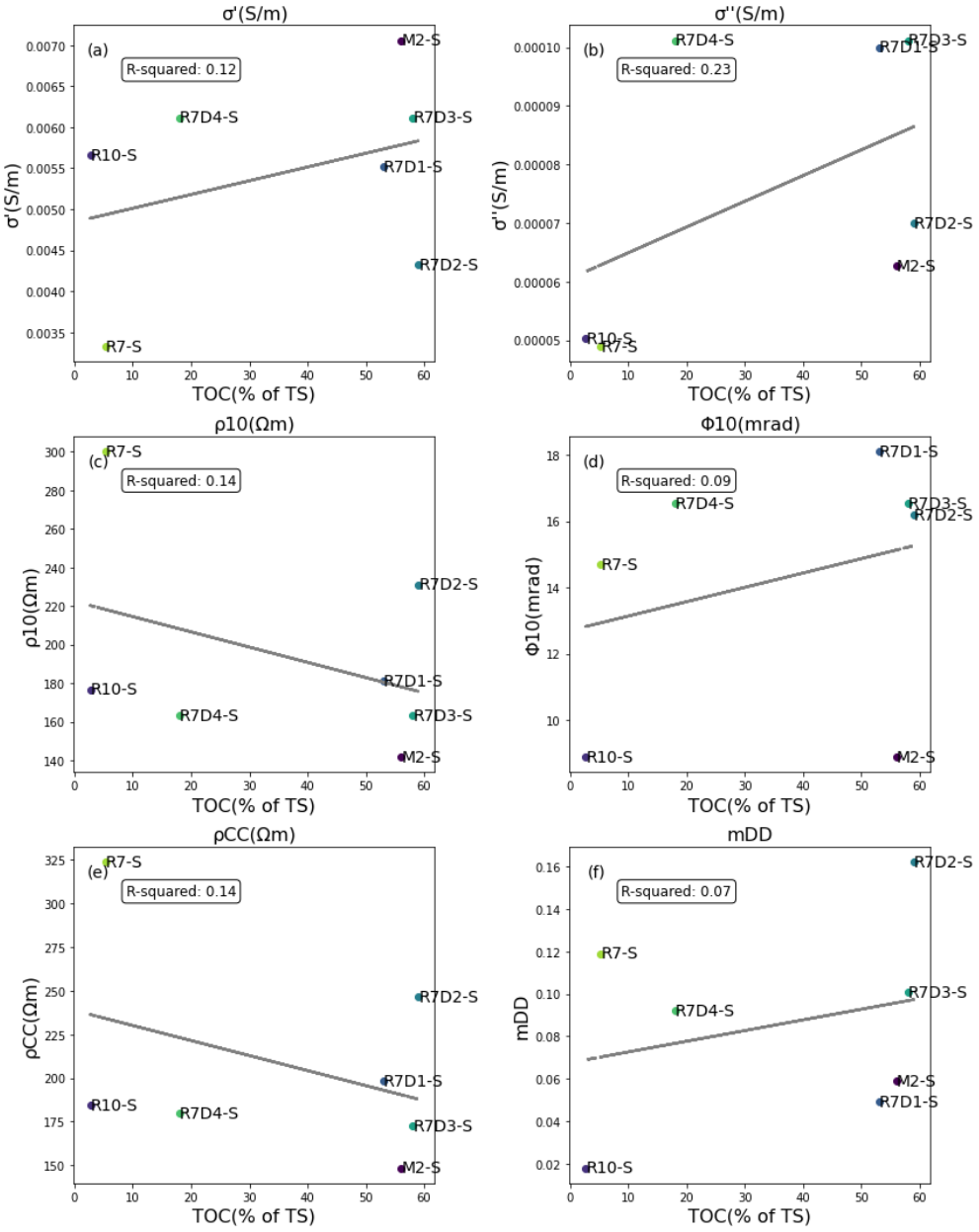

Figure 8: Different parameters of SIP analysis with respect to TOC for sediment sample. Here, a) σ' is real part of conductivity, b) σ'' is imaginary part of conductivity, c) ρ_{10} is resistivity at 10 Hz, d) φ_{10} is (-) phase shift at 10 Hz, e) ρ_{cc} is Cole-Cole resistivity, and f) m_{DD} is Debye-Decomposition chargeability vs TOC (% of Total Solids)

4.3.2 Fe vs SIP parameters of Sediment Sample

Like the comparison of TOC , Iron (Fe) is also showing a disperse data. All compared parameters have very low R^2 values and no relationship can be seen either. Figure 9 is showing the plots against Fe and measured sediment values.

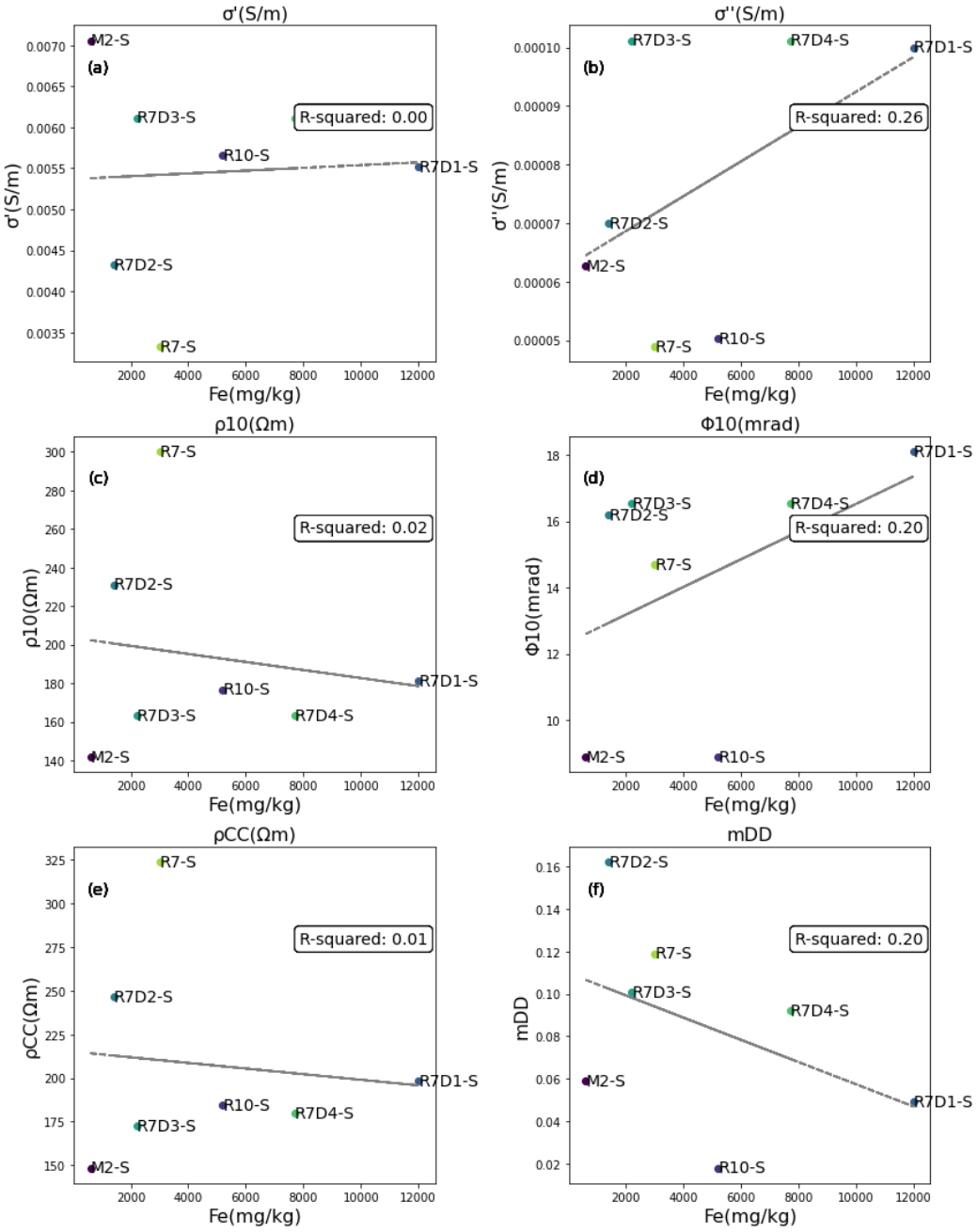

Figure 9: Different parameters of SIP analysis with respect to Fe for sediment sample. Here, a) σ' is real part of conductivity, b) σ'' is imaginary part of conductivity, c) ρ_{10} is resistivity at 10 Hz, d) φ_{10} is (-) phase shift at 10 Hz, e) ρ_{cc} is Cole-Cole resistivity, and f) m_{DD} is Debye-Decomposition chargeability vs Fe (mg/kg)

4.3.3 Porosity and SIP parameters of Sediment Sample

The porosity within the sample holder has been calculated by the mentioned methods in 3.2.2.4 and plotted against the SIP parameters for sediment samples for sediment sample. No significant relationship can be seen with porosity and measured SIP parameters, although chargeability

is showing 0.5 as the coefficient of variation. Figure 10 is showing the plotted data and trends with porosity. Table 5 is showing the calculated porosity by Archie's Law (Archie, 1942). It is important to mention that, the porosity showing in Table 5 is a measurement inside the sample holder. As the soil sample was fully saturated and consisted of peat, the porosity values are high.

Table 5: Calculated Porosity from formation factor by Archie's law

Sample	**Formation factor**	**Porosity (%)**
M2-S	1.25	89.44
R10-S	2.48	63.50
R7D1-S	2.18	67.78
R7D2-S	1.3	87.80
R7D3-S	1.16	92.67
R7D4-S	1.17	92.52
R7-S	1.24	89.97

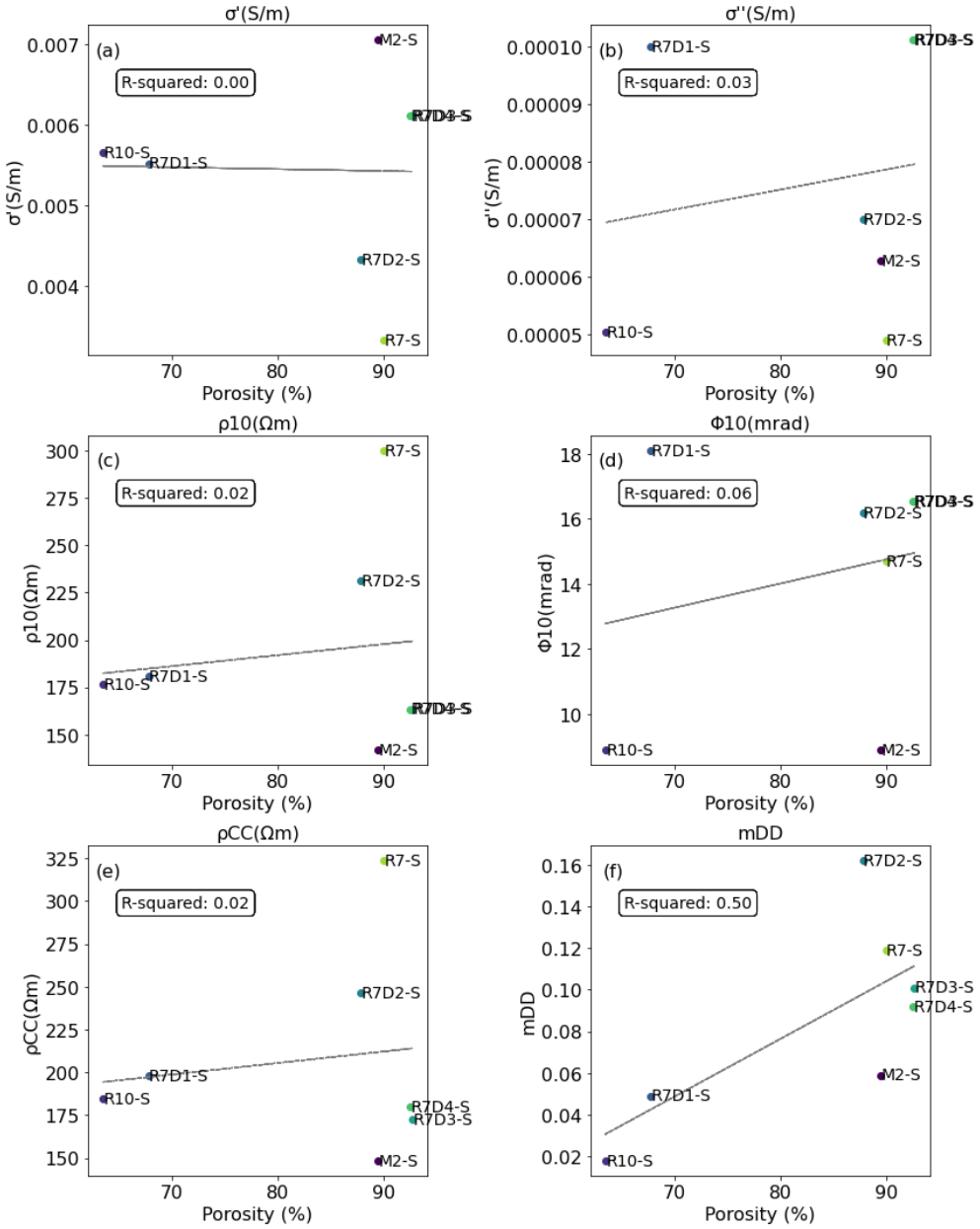

Figure 10: Different parameters of SIP analysis with respect to Porosity for sediment sample. Here, a) σ' is real part of conductivity, b) σ'' is imaginary part of conductivity, c) ρ_{10} is resistivity at 10 Hz, d) φ_{10} is (-) phase shift at 10 Hz, e) ρ_{cc} is Cole-Cole resistivity, and f) m_{DD} is Debye-Decomposition chargeability vs Porosity (%)

4.4 Comparison of NOM and SIP parameters for water samples

In this section SIP parameters are compared with water sample including TOC, Fe, pH, turbidity, dissolved oxygen, and color. Although it is important to mention that, TOC and Fe values used in this section for comparison are obtained from sediment samples and not from water

samples. Since the top layer sediment has been used, it may have some influences on the water too. The results for the selected water parameters with respect to SIP measured data are stated below.

4.4.1 TOC vs SIP parameters of Water Sample

In Figure 11 the SIP parameter of water sample with respect to TOC are shown. For water sample imaginary part of conductivity, and negative phase shift are nearly zero. Those values are not suitable to develop correlation. Apart from those, other parameters, like resistivity and chargeability, are not showing any significant correlation.

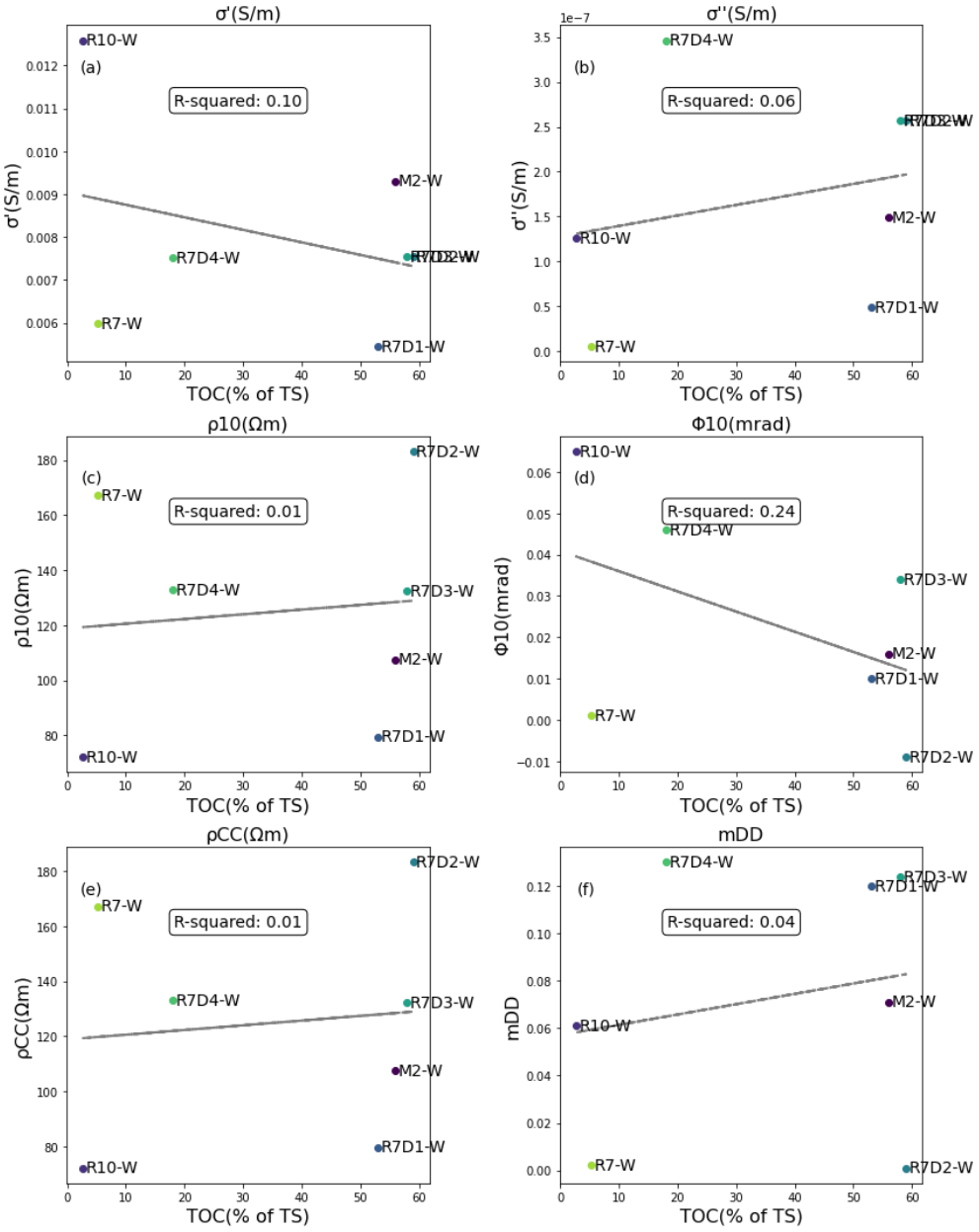

Figure 11: Different parameters of SIP analysis with respect to TOC for water sample. Here, a) σ' is real part of conductivity, b) σ'' is imaginary part of conductivity, c) ρ_{10} is resistivity at 10 Hz, d) φ_{10} is (-) phase shift at 10 Hz, e) ρ_{cc} is Cole-Cole resistivity, and f) m_{DD} is Debye-Decomposition chargeability vs TOC (% of Total Solids)

4.4.2 Fe vs SIP parameters of Water Sample

Comparing the SIP parameters with Fe values shows weak correlation with chargeability and resistivity about 0.29 and 0.3 in Figure 12. If this result is compared with the sediment analysis from section 4.3.2 (Figure 9f) it can be seen that, chargeability is showing different trends.

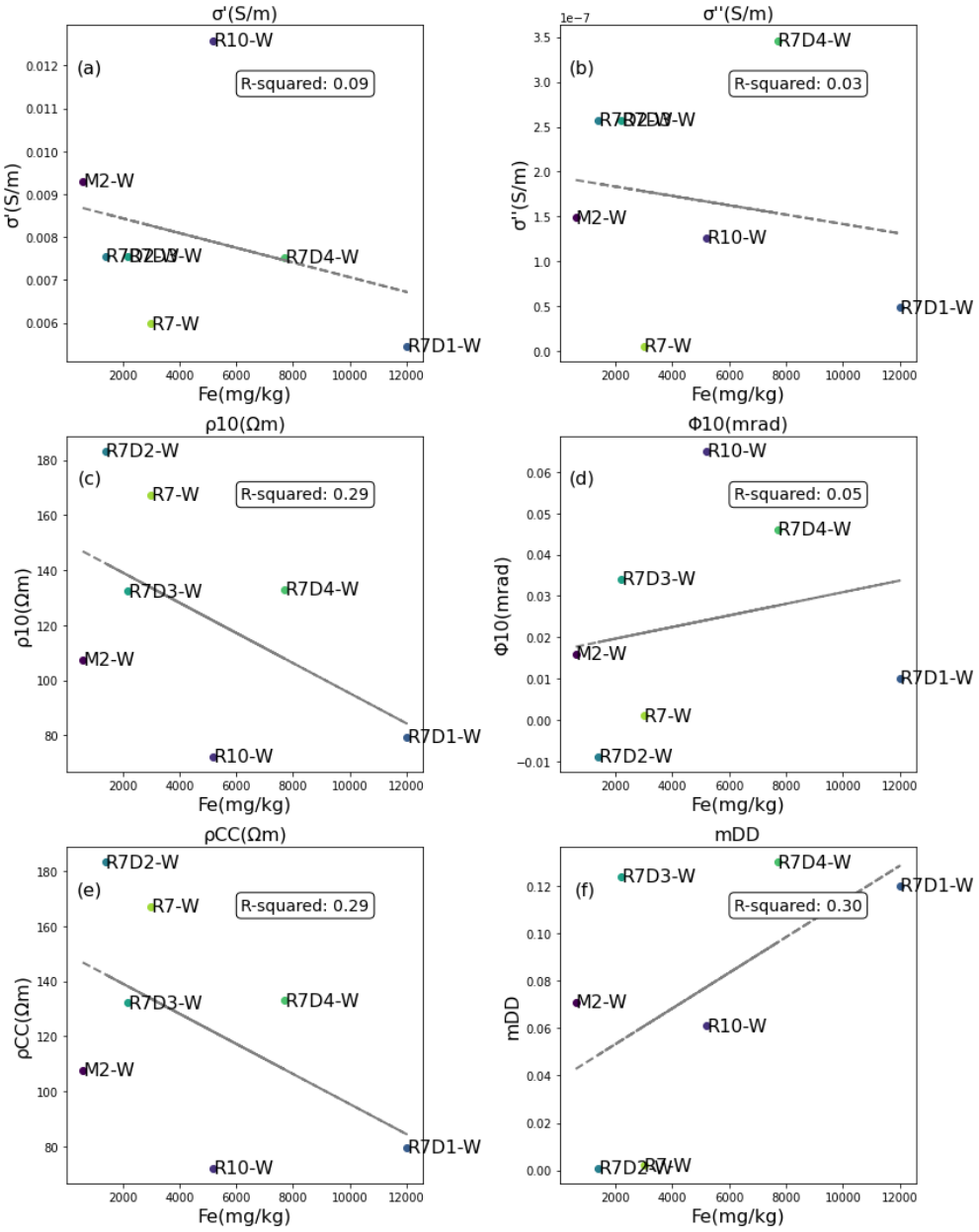

Figure 12: Different parameters of SIP analysis with respect to Fe for water sample. Here, a) σ' is real part of conductivity, b) σ'' is imaginary part of conductivity, c) ρ_{10} is resistivity at 10 Hz, d) φ_{10} is (-) phase shift at 10 Hz, e) ρ_{cc} is Cole-Cole resistivity, and f) m_{DD} is Debye-Decomposition chargeability vs Fe (mg/kg)

4.4.3 Dissolved Oxygen vs SIP parameters of Water Sample

SIP parameters have been compared with Dissolved oxygen (DO) data from the field. The results obtained here is showed best fit with real part of conductivity, imaginary part of conductivity, and chargeability. The corresponding R^2 values lies between 0.19-0.32 for real part of conductivity, imaginary conductivity and chargeability and no correlation can be

seen with other parameters.

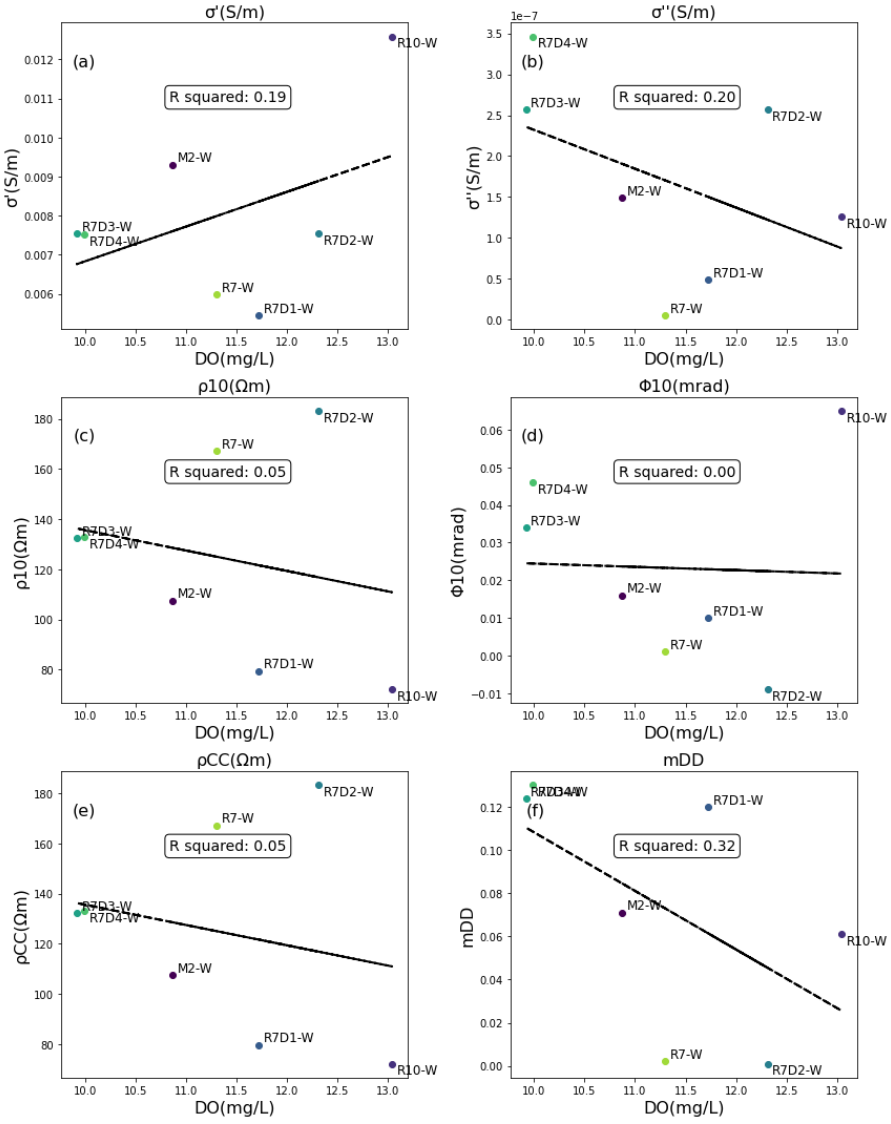

Figure 13: Different parameters of SIP analysis with respect to DO for water sample. Here, a) σ' is real part of conductivity, b) σ'' is imaginary part of conductivity, c) ρ_{10} is resistivity at 10 Hz, d) φ_{10} is (-) phase shift at 10 Hz, e) ρ_{cc} is Cole-Cole resistivity, and f) m_{DD} is Debye-Decomposition chargeability vs DO (mg/L)

4.4.4 Turbidity vs SIP parameters of Water Sample

The measured turbidity of the water sample does not show any significant correlation with the SIP data. As shown in Figure 14, the data are actually dispersed. Only chargeability shows a relatively higher R^2 value of 0.39.

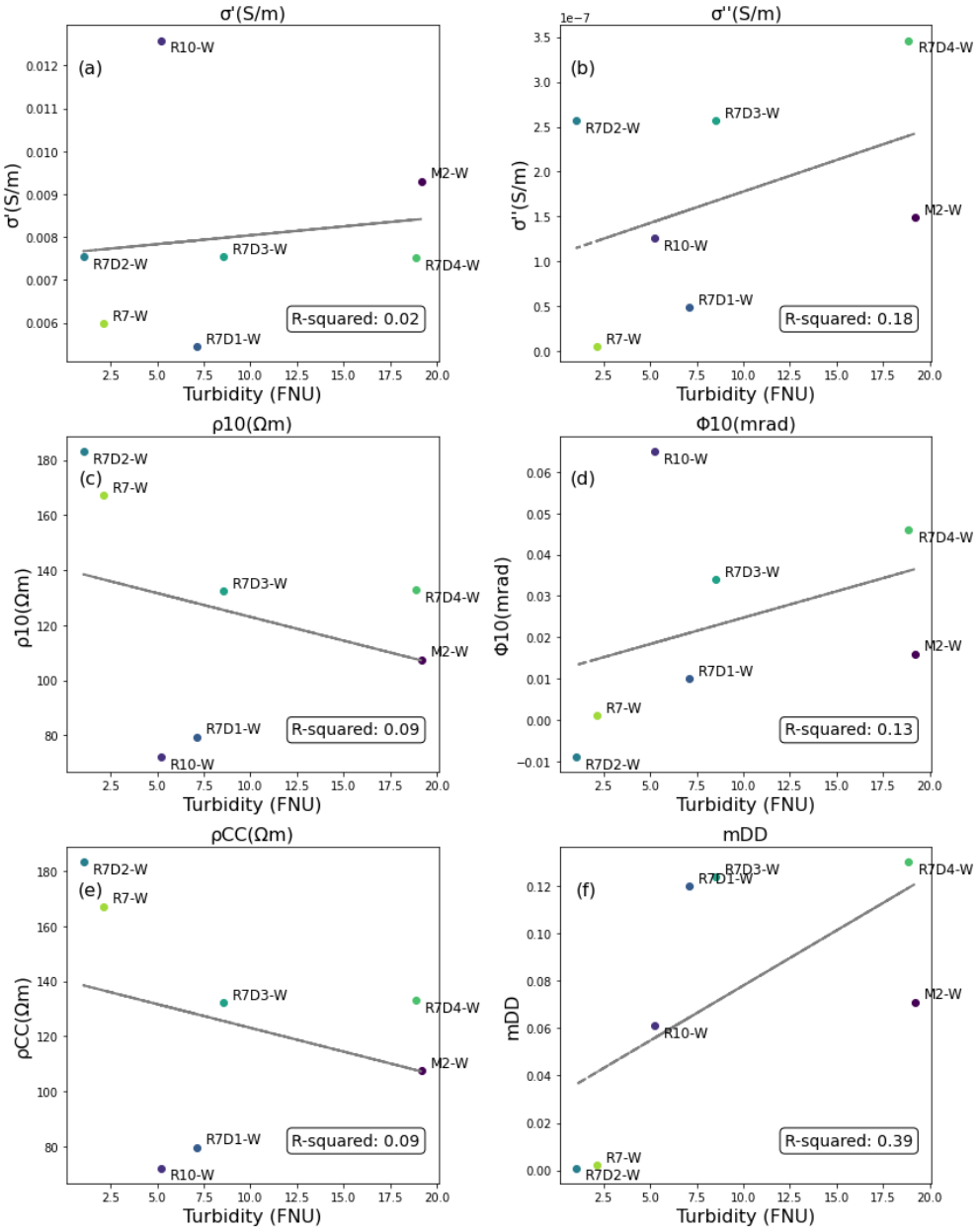

Figure 14: Different parameters of SIP analysis with respect to Turbidity for water sample. Here, a) σ' is real part of conductivity, b) σ'' is imaginary part of conductivity, c) ρ_{10} is resistivity at 10 Hz, d) φ_{10} is (-) phase shift at 10 Hz, e) ρ_{cc} is Cole-Cole resistivity, and f) m_{DD} is Debye-Decomposition chargeability vs Turbidity (FNU)

4.4.5 Water Color vs SIP parameters of Water Sample

In Figure 15 the water color is plotted against different SIP parameters. For imaginary conductivity a slight downward trend can be observed with coefficient of correlation values about 0.39. For other SIP parameters no correlation could be observed.

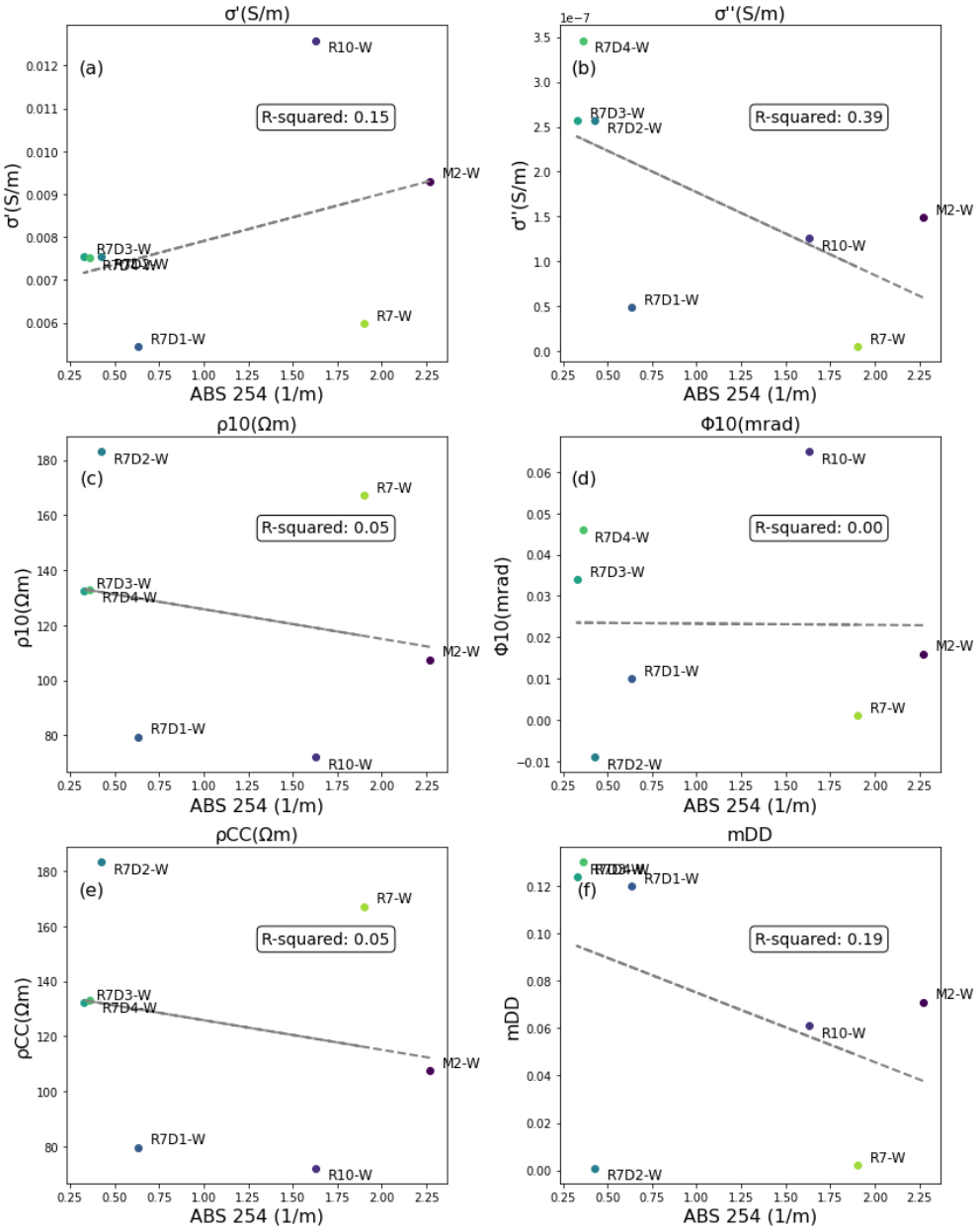

Figure 15: Different parameters of SIP analysis with respect to water color for water sample. Here, a) σ' is real part of conductivity, b) σ'' is imaginary part of conductivity, c) ρ_{10} is resistivity at 10 Hz, d) φ_{10} is (-) phase shift at 10 Hz, e) ρ_{cc} is Cole-Cole resistivity, and f) m_{DD} is Debye-Decomposition chargeability vs water color measured in ABS 254 (1/m)

4.4.6 pH vs SIP parameters of Water Sample

The pH of the water is plotted against the SIP parameter in Figure 16. R^2 values of 0.53 and 0.45 can be seen for imaginary conductivity and chargeability. However, no correlation can be seen with other SIP parameters.

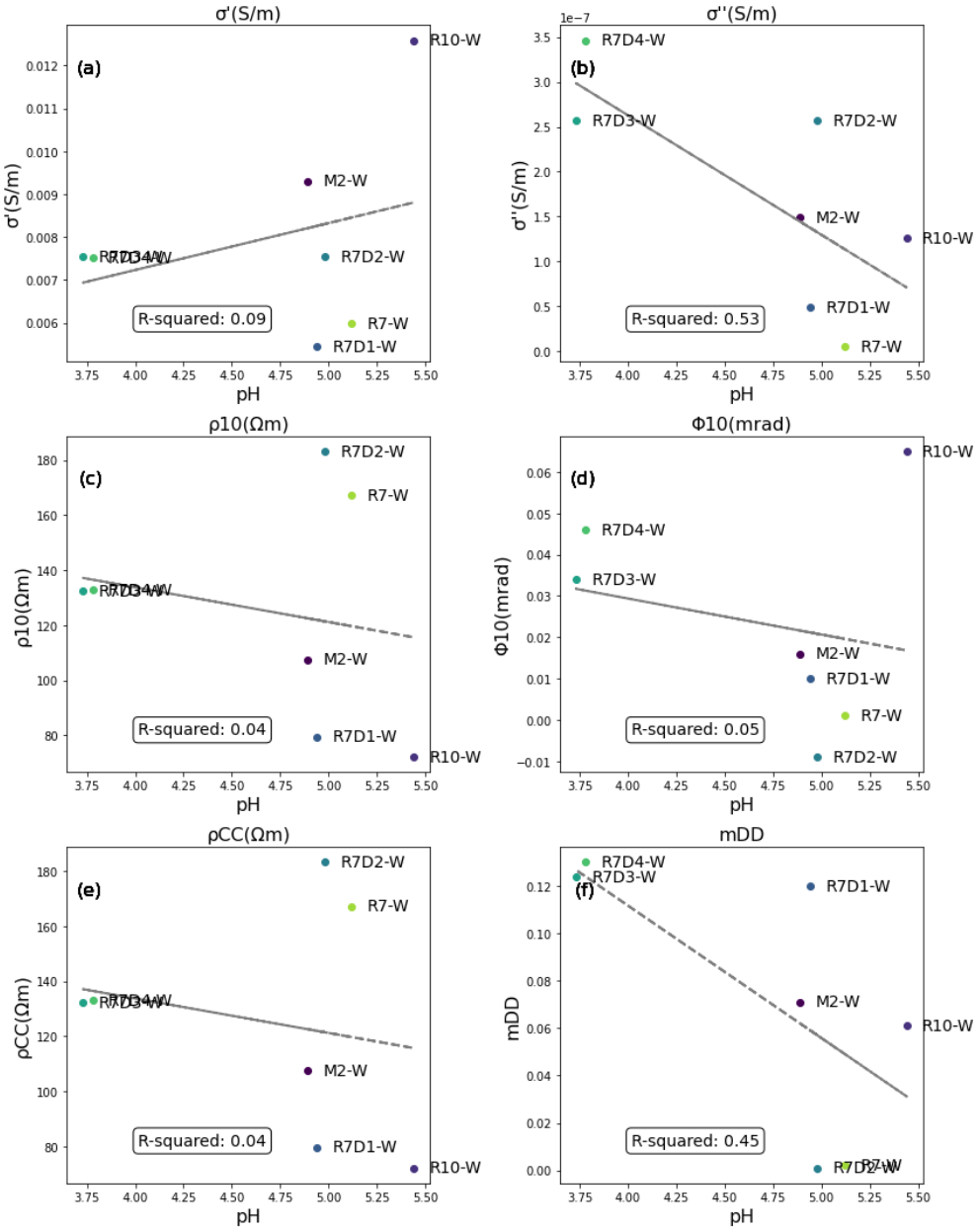

Figure 16: Different parameters of SIP analysis with respect to pH os water sample. Here, a) σ' is real part of conductivity, b) σ'' is imaginary part of conductivity, c) ρ_{10} is resistivity at 10 Hz, d) φ_{10} is (-) phase shift at 10 Hz, e) ρ_{cc} is Cole-Cole resistivity, and f) m_{DD} is Debye-Decomposition chargeability vs pH

5. Discussion

5.1 Spectral properties of SIP and correlation for sediment and water samples

In this study 7 sediment samples and 7 water samples were collected and measured with SIP analysis and laboratory analysis. Water samples typically have high conductivity compared to other materials such as sediments (US EPA, 2012). Therefore, in Figure 4, all sediment samples show higher resistivity than water. This result is also inline with previous studies by Rahman et al. (2014) and Lagabrielle (1983). Sediment resistivity should be higher than water, as the solid particle creates a barrier for the current to flow. However, sediment sample M2-S has shown low sediment resistivity which is unexpected. The presence of moisture or water can significantly reduce the resistive behavior of soil samples (Pozdnyakov et al., 2006). As the sediment samples were fully saturated, it decreased the resistivity of the sediment significantly. Change in resistivity between samples could also be caused by the sediments' soil type and are therefore location-dependent. The underlying soil of location R7 is glacial deposits, and R10, R7-Ditches (R7-D1, R7-D2, R7-D3, R7-D4) are mainly peatland according to (Geological Survey of Sweden, 2024). In Figure 6a, it is evident that R7-S and R7D2-S has a higher value of resistivity, whereas R7D1-S, R7D3-S, R7D4-S, R10-S and M2-S are subjected to low resistivity.

When looking at Figure 6b, it can be seen that the sediment samples exhibit a peak in their phase shift around 30-40 Hz. This effect is most pronounced for the R7-Ditches sample. In contrast, the water sample in Figure 7b shows a negligible phase shift. This suggests that the sediment samples are more susceptible to electrical polarization compared to the water sample.

Sediment samples in Figure 8 have shown some slight correlation between TOC and imaginary conductivity. This increasing trend has also been confirmed before with a controlled experiment by Strobel et al. (2023). In their study, experiments on both real field samples and artificial mixtures of peat and sand has been conducted. They found a direct relationship between TOC content and the imaginary part of conductivity with a R^2 value of 0.95. They also noted that an increase in TOC content leads to a corresponding increase in the imaginary part of conductivity. Iron (Fe) in Figure 9 has also followed the same positive trends with imaginary conductivity for sediment sample. In contrast, chargeability is showing a negative trend with increasing iron content although both correlations are very weak. Chargeability of a material is mainly dependent on the

types of minerals present, grain size distribution, and mobility of ions in the pore fluid (Jones, 2018). Therefore the results for Fe and TOC are influenced by other factors as well. Presence of Fe mineral in sediment can decrease the resistivity, as shown in Figure 9e, which is caused by increase in metalic particles, that lead to high electronic conductivity.

When a material is subjected to polarization, its pore space narrows due to the formation of stern and diffuse layers (Bücker et al., 2019). In that case, the charges cannot travel easily. Therefore, a smaller pore space leads to a larger accumulation of charges, which in turn results in higher chargeability. This phenomenon can not be depicted in Figure 10f, which shows a linear upward trend with porosity and chargeability, which is not expected.

The correlation plot between TOC and SIP measurements of water samples in Figure 11 did not show any significant relationship due to the fact that, the TOC measurements are actually from the sediment sample. For water sample the imaginary part of conductivity and negative phase shift is nearly zero, and correlation found in Figure 11 are also very weak. Same goes for Fe and SIP measurements of water samples in Figure 12. No significant relation can be seen for TOC and Fe of water samples. DO, turbidity, pH, and color showed some relationship with SIP signals, with both positive and negative trends. When assessing DO and SIP data, it can be seen in Figure 13b,e,f that imaginary conductivity, resistivity, and chargeability have downward trend. DO is responsible for oxidation and reduction potential in water along with aerobic respiration (Boyd, 2000) and it is also temperature dependent (US EPA, 2024; Walczyńska & Sobczyk, 2017). Hence, increase in DO will result in increase in resistivity, which is different than the result obtained from Figure 13e. Therefore the trends seen in all the above mentioned figures are very uncertain due to the limitations of data points and no correlation could be seen here as well.

Results from the turbidity of water (Figure 14) and SIP signals show a weak relation with imaginary conductivity. This phenomenon could be described as the presence of colloidal particles in water. The colloidal particles in water could potentially make the water more conductive, hence increasing conductivity with increased turbidity in the water. Colloidal particles can also hold charges in water which could potentially increase the chargeability with turbidity.

During sample collection, the water at location M2 was optically browner than other locations. It can be seen from Figure 6a that M2-S is showing less resistivity. Water with a high brown color is dependent on several long-term and short-term factors, as shown by Klante et al. (2021), but it is also due to the leaching of humic substances present in forest streams

(Löfgren et al., 2003), that can results in decrease of resistivity. In Figure 15e the resistivity of water sample is also decreasing with increasing water color. However, this trend can not be confirmed, as the data is uncertain. Therefore, water color with respect to the SIP signal cannot provide any direct information (Figure 15) and it can not be directly determined from SIP signals alone. This statement is also valid for water pH, which follows the same pattern as shown in Figure 16. Accordingly, no correlation can be observed here as well.

5.2 Uncertainty in Data Measurements

Although some weak correlations can be seen between NOM in sediment and SIP signals, they are uncertain. The reason for this uncertainty stems from the variation in sampling locations and the use of only the top sediment for sample preparation. Uncontrolled sample condition could also be an issue, as the sample didn't go through any kind of filtering. Sample used in this research are too heterogeneous for location dependency and number of samples are too small to find a good statistical relationship. So, comparatively large data points need to be included in further analysis, which eventually can give an understanding of SIP behavior. However, it is not certain that a large sample size can establish a relationship between NOM in sediment and SIP. Further research is needed to reach a definitive conclusion.

6. Conclusion

This study has focused on analyzing the spectral induced polarization (SIP) of sediment and water samples to identify connections between the concentration of natural organic matter (NOM) and SIP signals. After conducting a thorough investigation, it is found that no correlation between NOM in sediment and SIP signal exists, considering the uncertainties in this research.

Upon analyzing the general qualities, it is observed that water and sediment samples exhibited different behaviors. Water consistently showed small phase changes, whereas sediment has higher resistivity. These observations are consistent with previous studies, which strengthens the credibility of the findings. In addition, the analysis of the relationship between NOM and SIP measured data of sediment samples revealed no significant patterns except a very weak relation between TOC and imaginary conductivity. Nevertheless, there are uncertainties caused by fluctuations in the sampling process. When examining the connection between NOM with SIP measured data of water sample, no direct correlation can be found. Although turbidity shows limited correlations with SIP signals, dissolved oxygen (DO) exhibited contradictory patterns, highlighting the complex nature of water chemistry. Efforts to establish a correlation between NOM in sediment and SIP measurements have been unsuccessful in finding definitive relationships. This is mostly because of the heterogeneous samples and variations in sample size.

In the future, a more comprehensive approach can be achieved by incorporating additional data points into the study and integrating them with other geophysical testing methods. This combined approach would provide a more robust verification of the results. Additionally, investigating the relationship between a wider range of chemical parameters and the SIP parameters would be beneficial. Finally, conducting the study with controlled samples would allow for a more precise identification of any discrepancies or limitations in the current methodology.

In summary, this study shows preliminary results from field sample using spectral induced polarization signals as indicators for specific sediment characteristics. However, it also highlights the need for further research to address existing limitations and refine understanding. Future research should focus on increasing the number of data points, ensuring proper control of sample conditions, and utilizing advanced analytical tools to better understand the complex details of NOM-SIP connections. Moreover, this could potentially lead to a better understanding of the brownification process with necessary monitoring and evaluation.

References

Archie, G. (1942). The Electrical Resistivity Log as an Aid in Determining Some Reservoir Characteristics. *Transactions of the AIME*, *146*(01), 54–62. https://doi.org/10.2118/942054-G

Arora, P. (2017, April). Physical, Chemical and Biological Characteristics of Water (e Content Module). In *Water resources and management*. https://ebooks.inflibnet.ac.in/esp05/chapter/physical-chemical-and-biological-characteristics-of-water/ (Accessed 2024-03-02)

Atlas Scientific. (2024). What Is The Typical Water Conductivity Range? — Atlas Scientific. https://atlas-scientific.com/blog/water-conductivity-range/

Bartosiewicz, M., Przytulska, A., Lapierre, J.-F., Laurion, I., Lehmann, M. F., & Maranger, R. (2019). Hot tops, cold bottoms: Synergistic climate warming and shielding effects increase carbon burial in lakes. *Limnology and Oceanography Letters*, *4*(5), 132–144. https://doi.org/10.1002/lol2.10117

Birge, E. A. (A. (1922). A second report on limnological apparatus. *(No Title)*, *20*, 533–552. https://cir.nii.ac.jp/crid/1130000797128098048

Borgström, A. (2020). *Lake Bolmen Past, present and future* (tech. rep.). https://forskningsstationbolmen.se/app/uploads/Bolmen-Report.pdf

Boyd, C. E. (2000). Dissolved Oxygen and Redox Potential. In *Water quality: An introduction* (pp. 69–94). Springer US. https://doi.org/10.1007/978-1-4615-4485-25

Bozorg-Haddad, O., Delpasand, M., & Loáiciga, H. A. (2021). 10 - Water quality, hygiene, and health. In O. Bozorg-Haddad (Ed.), *Economical, political, and social issues in water resources* (pp. 217–257). Elsevier. https://doi.org/https://doi.org/10.1016/B978-0-323-90567-1.00008-5

Bücker, M., Flores Orozco, A., Undorf, S., & Kemna, A. (2019). On the Role of Stern- and Diffuse-Layer Polarization Mechanisms in Porous Media. *Journal of Geophysical Research: Solid Earth*, *124*(6), 5656–5677. https://doi.org/10.1029/2019JB017679

CEN. (2005). *Working draft 2nd consultation Solid materials-Microwave digestion of sediment, sludge, soil and biowaste for the extraction of nitric acid soluble fraction of trace elements*. https://horizontal.ecn.nl/docs/society/horizontal/STD6180_digestion_nitricacid.pdf

Cole, K. S., & Cole, R. H. (1941). Dispersion and Absorption in Dielectrics I. Alternating Current Characteristics. *The Journal of Chemical Physics*, *9*(4), 341–351. https://doi.org/10.1063/1.1750906

Cromphout, J., Verdickt, L., Martin, E., Vanhoucke, R., & Vanhullebusch, T. (2008). Comparison between magnetic ion exchange resin-ultrafiltration and enhanced coagulation–filtration for the treatment of an NOM

loaded surface water. *Water Science & Technology: Water Supply*, *8*. https://doi.org/10.2166/ws.2008.147

Davis, M. L., York, N., San, C., Lisbon, F., Madrid, L., City, M., New, M., San, D., Singapore, J. S., & Toronto, S. (2010). Water and wastewater engineering : design principles and practice. https://thuvienso.hoasen.edu.vn/handle/123456789/9253

Eklund, A., Mårtensson, J. A., Bergström, S., & Sjökvist, E. (2016). Framtidens vattentillgång i Mälaren Göta älv Bolmen Vombsjön och Gavleån. *KLIMATOLOGI Nr*, *39*.

Ekman, S. (1911). Neue Apparate zur qualitativen und quantitativen Erforschung der Bodenfauna der Seen. *Internationale Revue der gesamten Hydrobiologie und Hydrographie*, *3*(5-6), 553–561. https://doi.org/10.1002/IROH.19110030509

Ekström, S. (2013). Brownification of freshwaters - the role of dissolved organic matter and iron. http://lup.lub.lu.se/record/4076293

Elias, S. (2013). Geosciences: The Study of the Solid and Molten Parts of the Earth and How They Interact with Our Environment. In *Reference module in earth systems and environmental sciences*. Elsevier. https://doi.org/10.1016/B978-0-12-409548-9.05354-9

Estlander, S., Pippingsköld, E., & Horppila, J. (2021). Artificial ditching of catchments and brownification-connected water quality parameters of lakes. *Water Research*, *205*, 117674. https://doi.org/10.1016/J.WATRES.2021.117674

Finstad, A. G., Andersen, T., Larsen, S., Tominaga, K., Blumentrath, S., de Wit, H. A., Tømmervik, H., & Hessen, D. O. (2016). From greening to browning: Catchment vegetation development and reduced S-deposition promote organic carbon load on decadal time scales in Nordic lakes. *Scientific Reports*, *6*(1), 31944. https://doi.org/10.1038/srep31944

Frederick, K. D., & Major, D. C. (1997). Climate Change and Water Resources. *Climatic Change*, *37*(1), 7–23. https://doi.org/10.1023/A:1005336924908

Gadmar, T. C., Vogt, R. D., & Østerhus, B. (2002). The Merits of the High-temperature Combustion Method for Determining the Amount of Natural Organic Carbon in Surface Freshwater Samples. *International Journal of Environmental Analytical Chemistry*, *82*(7), 451–461. https://doi.org/10.1080/0306731021000018099

Geological Survey of Sweden. (2024). SGU's Map Viewer. https://apps.sgu.se/kartvisare/kartvisare-jordarter-25-100.html (Accessed 2024-03-10)

Göta älvs vattenvårdsförbund. (2016). Conductivity - Sweden's water-richest river. https://www.gotaalvvvf.org/resultat/begreppsforklaringar/konduktivitet.4.271d6b7512e53cf0cf98000910.html

Härkönen, L. H., Lepistö, A., Sarkkola, S., Kortelainen, P., & Räike, A. (2023). Reviewing peatland forestry: Implications and mitigation measures for freshwater ecosystem browning. *Forest Ecology and*

Management, *531*, 120776. https://doi.org/10.1016/J.FORECO.2023.120776

Hermans, T., Nguyen, F., Robert, T., & Revil, A. (2014). Geophysical Methods for Monitoring Temperature Changes in Shallow Low Enthalpy Geothermal Systems. *Energies*, *7*(8), 5083–5118. https://doi.org/10.3390/en7085083

Houser, J. N. (2006). Water color affects the stratification, surface temperature, heat content, and mean epilimnetic irradiance of small lakes. *Canadian Journal of Fisheries and Aquatic Sciences*, *63*(11), 2447–2455. https://doi.org/10.1139/f06-131

Jones, F. (2018). UBC Earth and Ocean Sciences: Chargeability. https://www.eoas.ubc.ca/courses/eosc350/content/foundations/properties/2physprop-iag.htm

Karlsson, T., & Persson, P. (2012). Complexes with aquatic organic matter suppress hydrolysis and precipitation of Fe(III). *Chemical Geology*, *322-323*, 19–27. https://doi.org/10.1016/j.chemgeo.2012.06.003

KC Denmark. (2022). Kajak Model B, KC Denmark · Oceanography · Limnology · Hydrobiology. https://www.kc-denmark.dk/products/sediment-samplers/kajak-corer/kajak-model-b.aspx

Klante, C., Hägg, K., & Larson, M. (2022). Understanding short-term organic matter fluctuations to optimize drinking water treatment. *Water Practice and Technology*, *17*(10), 2141–2159. https://doi.org/10.2166/WPT.2022.121/1125892/WPT2022121.PDF

Klante, C., Larson, M., & Persson, K. M. (2021). Brownification in Lake Bolmen, Sweden, and its relationship to natural and human-induced changes. *Journal of Hydrology: Regional Studies*, *36*, 100863. https://doi.org/10.1016/J.EJRH.2021.100863

Knap-Bałdyga, A., & Żubrowska-Sudoł, M. (2023). Natural Organic Matter Removal in Surface Water Treatment via Coagulation—Current Issues, Potential Solutions, and New Findings. *Sustainability 2023, Vol. 15, Page 13853*, *15*(18), 13853. https://doi.org/10.3390/SU151813853

Knoll, L. B., Williamson, C. E., Pilla, R. M., Leach, T. H., Brentrup, J. A., & Fisher, T. J. (2018). Browning-related oxygen depletion in an oligotrophic lake. *Inland Waters*. https://doi.org/10.1080/20442041.2018.1452355

Köhler, S. J. (1999). Quantifying the role of natural organic acids on pH and buffering in Swedish surface waters. https://api.semanticscholar.org/CorpusID:99800431

Kritzberg, E. S., & Ekström, S. M. (2012). Increasing iron concentrations in surface waters - A factor behind brownification? *Biogeosciences*, *9*(4), 1465–1478. https://doi.org/10.5194/BG-9-1465-2012

Kritzberg, E. S. (2017). Centennial-long trends of lake browning show major effect of afforestation. *Limnology and Oceanography Letters*, *2*(4), 105–112. https://doi.org/10.1002/lol2.10041

Kruschwitz, S., Binley, A., Lesmes, D., & Elshenawy, A. (2010). Textural controls on low-frequency electrical spectra of porous media. *GEOPHYSICS*, *75*(4), WA113–WA123. https://doi.org/10.1190/1.3479835

Lagabrielle, R. (1983). The effect of water on direct current resistivity measurement from the sea, river or lake floor. *Geoexploration*, *21*(2), 165–170. https://doi.org/https://doi.org/10.1016/0016-7142(83)90006-6

Larsen, S., Andersen, T., & Hessen, D. O. (2011). Climate change predicted to cause severe increase of organic carbon in lakes. *Global Change Biology*, *17*(2), 1186–1192. https://doi.org/10.1111/j.1365-2486.2010.02257.x

Löfgren, S., Forsius, M., & Andersen, T. (2003). Climate induced water color increase in Nordic lakes and streams due to humus The color of water. http://info1.ma.slu.se/ima/publikationer/brochure/The_color_of_water.pdf

Martin, T., Günther, T., Weller, A., & Kuhn, K. (2021). Classification of slag material by spectral induced polarization laboratory and field measurements. *Journal of Applied Geophysics*, *194*, 104439. https://doi.org/https://doi.org/10.1016/j.jappgeo.2021.104439

Mehran, A., AghaKouchak, A., Nakhjiri, N., Stewardson, M. J., Peel, M. C., Phillips, T. J., Wada, Y., & Ravalico, J. K. (2017). Compounding Impacts of Human-Induced Water Stress and Climate Change on Water Availability. *Scientific Reports*, *7*(1), 6282. https://doi.org/10.1038/s41598-017-06765-0

Meyer-Jacob, C., Tolu, J., Bigler, C., Yang, H., & Bindler, R. (2015). Early land use and centennial scale changes in lake-water organic carbon prior to contemporary monitoring. *Proceedings of the National Academy of Sciences*, *112*(21), 6579–6584. https://doi.org/10.1073/pnas.1501505112

Nordsiek, S., & Weller, A. (2008). A new approach to fitting induced-polarization spectra. *Geophysics*, *73*, F235. https://doi.org/10.1190/1.2987412

Ontash & Ermac. (n.d.). Ontash & Ermac - Products. https://www.ontash.com/products.htm#PSIP (Accessed 2024-04-08)

Pal, M., Samal, N., Roy, P., & Biswas Roy, M. (2015). Electrical Conductivity of Lake Water as Environmental Monitoring –A Case study of Rudra sagar Lake. *Journal of Environmental Science,Toxicology and Food Technology*.

Pozdnyakov, A. I., Pozdnyakova, L. A., & Karpachevskii, L. O. (2006). Relationship between water tension and electrical resistivity in soils. *Eurasian Soil Science*, *39*(1), S78–S83. https://doi.org/10.1134/S1064229306130138

Rahman, M., Wong, Y. S., & Nguyen, M. D. (2014). 11.06 - Compound and Hybrid Micromachining: Part II – Hybrid Micro-EDM and Micro-ECM. In S. Hashmi, G. F. Batalha, C. J. Van Tyne, & B.

Yilbas (Eds.), *Comprehensive materials processing* (pp. 113–150). Elsevier. https://doi.org/https://doi.org/10.1016/B978-0-08-096532-1.01329-7

Revil, A., Koch, K., & Holliger, K. (2012). Is it the grain size or the characteristic pore size that controls the induced polarization relaxation time of clean sands and sandstones? *Water Resources Research*, *48*. https://doi.org/10.1029/2011WR011561

Reynolds, J. M. (1997). *An introduction to applied and environmental geophysics*. Chichester ; New York : John Wiley, 1997. https://search.library.wisc.edu/catalog/999809641902121

Riyadh, A., & Peleato, N. M. (2024). Natural Organic Matter Character in Drinking Water Distribution Systems: A Review of Impacts on Water Quality and Characterization Techniques. *Water*, *16*(3), 446. https://doi.org/10.3390/w16030446

Rücker, C., Günther, T., & Wagner, F. M. (2017). pyGIMLi: An open-source library for modelling and inversion in geophysics. *Computers and Geosciences*, *109*, 106–123. https://doi.org/10.1016/j.cageo.2017.07.011

Secondi, J., Aumjaud, A., Pays, O., Boyer, S., Montembault, D., & Violleau, D. (2007). Water Turbidity Affects the Development of Sexual Morphology in the Palmate Newt. *Ethology*, *113*(7), 711–720. https://doi.org/10.1111/j.1439-0310.2007.01375.x

Sharma, P., Ofner, J., & Kappler, A. (2010). Formation of Binary and Ternary Colloids and Dissolved Complexes of Organic Matter, Fe and As. *Environmental Science & Technology*, *44*(12), 4479–4485. https://doi.org/10.1021/es100066s

Sillanpää, M., Matilainen, A., & Lahtinen, T. (2015). Chapter 2 - Characterization of NOM. In M. Sillanpää (Ed.), *Natural organic matter in water* (pp. 17–53). Butterworth-Heinemann. https://doi.org/https://doi.org/10.1016/B978-0-12-801503-2.00002-1

Strobel, C., Doerrich, M., Stieff, E.-H., Huisman, J. A., Cirpka, O. A., & Mellage, A. (2023). Organic Matter Matters—The Imaginary Conductivity of Sediments Rich in Solid Organic Carbon. *Geophysical Research Letters*, *50*(23). https://doi.org/10.1029/2023GL104630

Ström, E., & Karlsson Öhman, F. (2024). Brownification in a small stream originating from a peatland - A case study from Ryds Å in south Sweden. *TVVR 5000; (2024)*. http://lup.lub.lu.se/student-papers/record/9147476

Swedish Infrastructure for Ecosystem Science. (2023). Description of Lake Bolmen Location and lake information Sampling point. https://www.fieldsites.se/en-GB

Swedish Meteorological and Hydrological Institute. (2023). Model data per area — SMHI - Water web. https://vattenwebb.smhi.se/modelarea/ (Accessed 2024-05-20)

Swedish University of Agricultural Sciences. (2023). Turbidity/Haziness — Externwebben. https://www.slu.se/en/departments/aquatic-

sciences-assessment/laboratories/vattenlabb2/detaljerade-metodbeskrivningar/turbidityhaziness/(Accessed 2024-04-02)

Sydvatten AB. (2021). Our mission – Sydvatten. https://sydvatten.se/om-sydvatten/vart-uppdrag/ (Accessed 2024-04-27)

Sydvatten AB. (2024). Bolmen – Sydvatten. https://sydvatten.se/var-verksamhet/rapporter-om-ravattentakter/bolmen-3/ (Accessed 2024-05-02)

Thurman, E. M. (1985). *Organic Geochemistry of Natural Waters*. Springer Netherlands. https://doi.org/10.1007/978-94-009-5095-5/COVER

United Nation. (2023). Water is a common good not a commodity: UN experts — OHCHR. https://www.ohchr.org/en/statements-and-speeches/2023/03/water-common-good-not-commodity-un-experts (Accessed 2024-03-08)

US EPA. (2012). Conductivity. https://archive.epa.gov/water/archive/web/html/vms59.html (Accessed 2024-02-03)

US EPA. (2021). Turbidity; FACTSHEET ON WATER QUALITY PARAMETERS. https://www.epa.gov/system/files/documents/2021-07/parameter-factsheet_turbidity.pdf

US EPA. (2024). The Effect of Climate Change on Water Resources and Programs — Watershed Academy Web — US EPA. https://cfpub.epa.gov/watertrain/moduleFrame.cfm?parent_object_id=2456&object_id=2459 (Accessed 2024-02-07)

Walczyńska, A., & Sobczyk, Ł. (2017). The underestimated role of temperature–oxygen relationship in large-scale studies on size-to-temperature response. *Ecology and Evolution*, *7*(18). https://doi.org/10.1002/ece3.3263

Wang, C., & Slater, L. D. (2019). Extending accurate spectral induced polarization measurements into the kHz range: modelling and removal of errors from interactions between the parasitic capacitive coupling and the sample holder. *Geophysical Journal International*, *218*(2), 895–912. https://doi.org/10.1093/gji/ggz199

Water Information System Sweden. (2024). Bolmen - Sjö - VISS - VattenInformationsSystem för Sverige. https://viss.lansstyrelsen.se/Waters.aspx?waterMSCD=WA29456646

Weller, A., Slater, L., Nordsiek, S., & Ntarlagiannis, D. (2010). On the estimation of specific surface per unit pore volume from induced polarization: A robust empirical relation fits multiple data sets. *Geophysics*, *75*. https://doi.org/10.1190/1.3471577

Weyhenmeyer, G. A., Fröberg, M., Karltun, E., Khalili, M., Kothawala, D., Temnerud, J., & Tranvik, L. J. (2012). Selective decay of terrestrial organic carbon during transport from land to sea. *Global Change Biology*, *18*(1), 349–355. https://doi.org/10.1111/j.1365-2486.2011.02544.x

Winterdahl, M., Bishop, K., & Erlandsson, M. (2014). Acidification, Dissolved Organic Carbon (DOC) and Climate Change. In *Global environmental change* (pp. 281–287). Springer Netherlands. https://doi.org/10.1007/978-94-007-5784-4{_}107

YSI. (2024). Multiparameter Water Quality Sonde for Unattended Monitoring — ysi.com. https://www.ysi.com/exo2 (Accessed 2024-05-02)

Zaidi, J., & Pal, A. (2015). Influence of temperature on physico-chemical properties of freshwater ecosystem of bundelkhand region of uttar pradesh, india. *International Journal Of Current Research In Chemistry And Pharmaceutical Sciences*, *2*, 1–8.

Appendix A

Photos from field and laboratory

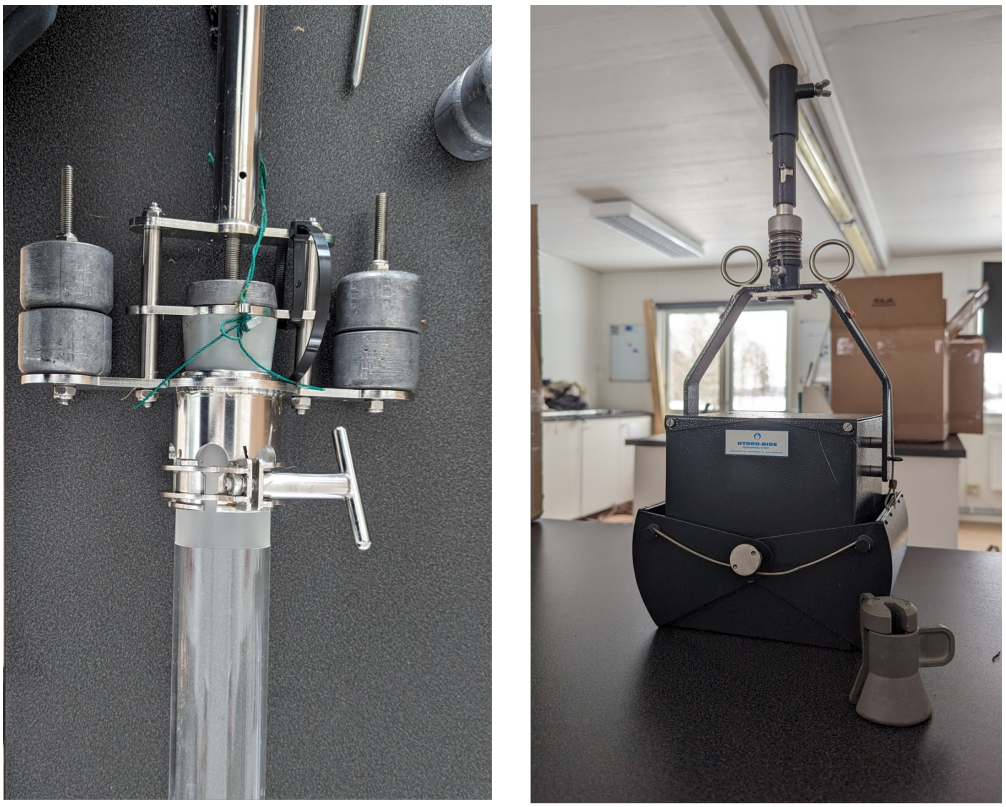

a) Kajak Sediment Sampler

b) Ekman-Birge Sediment Sampler

Figure 17: Sampler used for collecting sediment sample. Figure a) is showing Kajak Sediment Sampler and Figure b) is showing Ekman-Birge Sediment Sampler

Figure 18: Sample collection process of sediment from R7-D1 ditch. First and second picture is showing sample collection process and third picture is showing collected sediment column. The sampler using in this figure is Kajak Sediment Sampler.

Appendix B

Data inversion plot

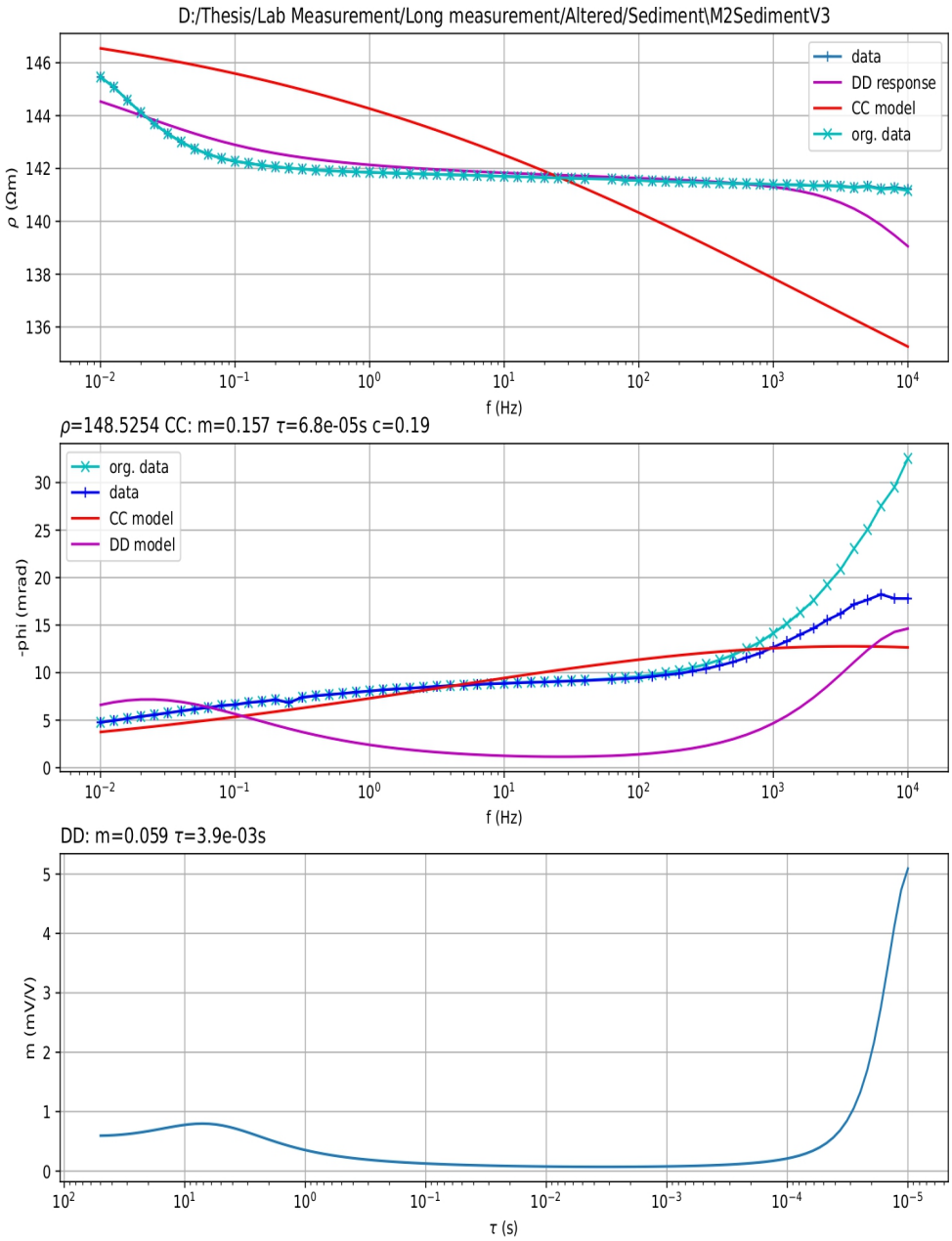

Figure 19: Results obtained from the pyGIMLi pacakage for sediment sample of M2 location. From top to bottom the first graph is showing fitted resistivity curve with measured SIP data, the second graph is showing fitted negative phase curve with measured SIP data. The third graph is showing chargeability vs relaxation time data for the fitted result. Here, CC means Cole-Cole model and DD means Debye Decomposition model.

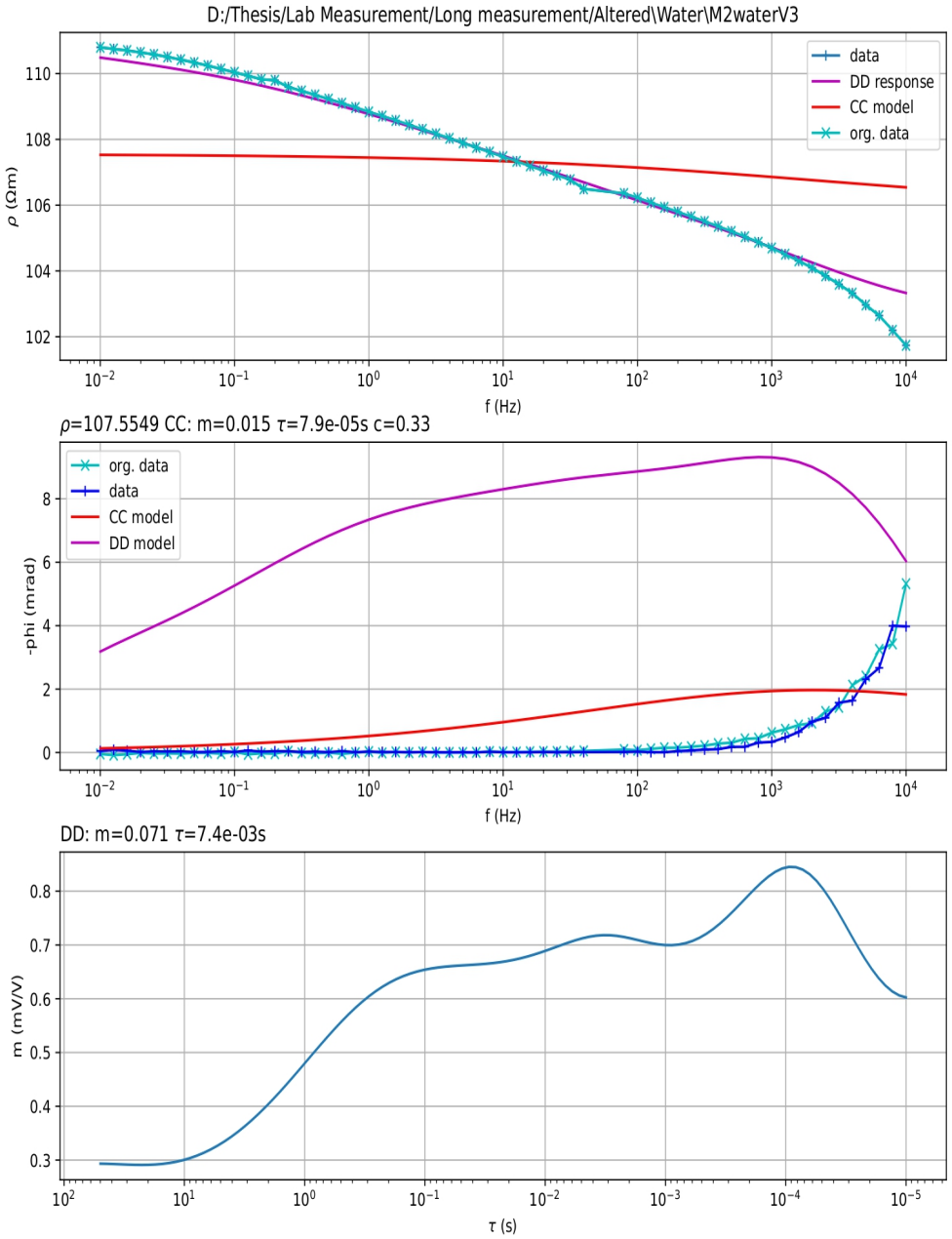

Figure 20: Results obtained from the pyGIMLi pacakage for sediment sample of M2 location. From top to bottom the first graph is showing fitted resistivity curve with measured SIP data, the second graph is showing fitted negative phase curve with measured SIP data. The third graph is showing chargeability vs relaxation time data for the fitted result. Here, CC means Cole-Cole model and DD means Debye Decomposition model.

Appendix C

Block Diagram

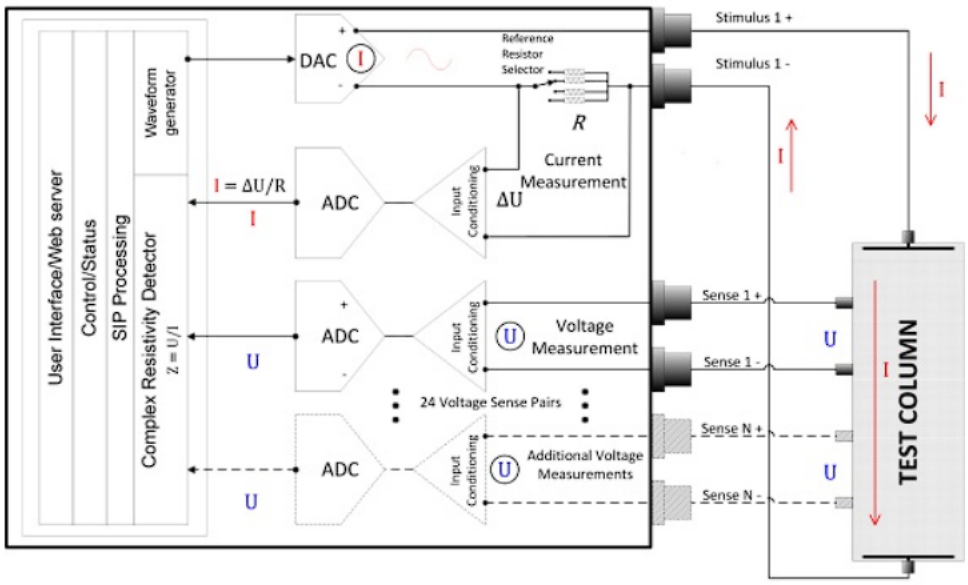

Figure 21: Block diagram of the Portable SIP unit used for the analysis. The figure is obtained from Ontash & Ermac (n.d.)